IEEE Access
Multidisciplinary | Rapid Review | Open Access Journal

Received August 31, 2020, accepted October 4, 2020, date of publication October 12, 2020, date of current version October 23, 2020.

Digital Object Identifier 10.1109/ACCESS.2020.3030221

UAV Relaying Enabled NOMA Network With Hybrid Duplexing and Multiple Antennas

DINH-THUAN DO[1], (Senior Member, IEEE), TU-TRINH THI NGUYEN[2], CHI-BAO LE[2], MIROSLAV VOZNAK[3], (Senior Member, IEEE), ZEESHAN KALEEM[4], AND KHALED M. RABIE[5], (Senior Member, IEEE)

[1]Wireless Communications Research Group, Faculty of Electrical & Electronics Engineering, Ton Duc Thang University, Ho Chi Minh City 700000, Vietnam
[2]Faculty of Electronics Technology, Industrial University of Ho Chi Minh City (IUH), Ho Chi Minh City 700000, Vietnam
[3]Department of Telecommunications, VSB Technical University of Ostrava, 70833 Ostrava, Czech Republic
[4]Department of Electrical and Computer Engineering, COMSATS University Islamabad, Wah Campus, Wah 47040, Pakistan
[5]Department of Engineering, Manchester Metropolitan University, Manchester M1 5GD, U.K.

Corresponding author: Dinh-Thuan Do (dodinhthuan@tdtu.edu.vn)

This work was supported by the Czech Ministry of Education, Youth, through the Institutional Grant SGS SP2020/65, conducted at the VSB-Technical University of Ostrava.

ABSTRACT This article studies the wireless systems by implementing the full-duplex (FD) unmanned aerial vehicle (UAV) relay to allow two nearby base stations joint communicate to distant users. The non-orthogonal multiple access (NOMA) assisted networks and design of multiple-antenna users are considered in order to improve the users' performance. To overcome obstacles in transmission environment, such a model of the uplink (UL) and the downlink (DL) relying on UAV relay is suitable to forward signals to far users. Moreover, practical scenario of imperfect successive interference cancellation (SIC) at each receiver is considered as main reason of degraded performance. To evaluate specific performance metric, we derive the closed-form expressions of outage probability. In addition, the throughput in delay-limited transmission mode of UAV relay assisted UL/DL NOMA system is also considered thoroughly. The derivations and results showed that the higher number of antennas at users could effectively improve the system throughput and reduce the outage probability. The numerical simulation results further indicate the effectiveness of the proposed system and the correctness of theoretical analysis.

INDEX TERMS Non-orthogonal multiple access, unmanned aerial vehicle, outage probability, throughput, full-duplex, imperfect SIC.

I. INTRODUCTION

As promising technology, non-orthogonal multiple access (NOMA) has been proposed to robust spectrum efficiency in next generation networks, where two important requirements include massive connectivity and reduced latency [1], [2]. Compared with the conventional orthogonal multiple access (OMA), multiple users are served with the same block of resources. The most important aspect of NOMA is that the users are allocated different power allocation factors. However, this leads to mutual interference imposed by other users and successive interference cancellation (SIC) which is required to mitigate such interference at the receivers [3]–[5]. Removing orthogonal characterization from the traditional OMA, the same time and frequency resources are shared among multiple NOMA users. With advantages of NOMA, it is relevant approach to provide advantages (massive connectivity and boost spectral efficiency) for Internet of Things (IoT) [6], [7]. According to the channel conditions, NOMA users are classified into two categories namely the far and the near users. However, quality of received signal at the far users may be varied from the near user [8]. To provide user fairness, more power is allocated to the far users which are admitted poor channel condition, while less power is assigned to those having good channel condition (the near users). However, to maintain the signal quality for the far users, the far users need be assigned the higher power levels. As a result, quality-of-service (QoS) requirement does not guarantee at the strong users (or near users), and hence lower reception reliability occurs at the

The associate editor coordinating the review of this manuscript and approving it for publication was Zhenhui Yuan.

weaker user [8]. Recently, to adopt a balance between the performance of the two users, several models of relaying architecture have been widely deployed into NOMA network. Several promising applications of NOMA are introduced recently, for example NOMA-aided ambient backscatter [9], and wireless powered networks are deployed to overcome the large scale fading between source and sink as well as achieve the green cooperative communications [10]. In other research, a dedicated relay is required to facilitate the transmission from the base station and the distant NOMA users under impacts of hardware impairments [11]–[13].

In simple approaches, half-duplex (HD) relays are employed in various kinds of networks [10]–[13]. Additional time resources is acquired in HD mode and this results in the degradation of spectral efficiency. In contrast, full-duplex (FD) scheme can be implemented to reduce loss of spectral efficiency [14], [15]. Unfortunately, inter-user interference and self-interference (SI) occur at the FD relay. In addition, such existing challenges are caused by FD mode in out-band relay systems, i.e. it can make a significant impact on the system performance. Several SI cancellation methods have been proposed to highlight the advantage of FD operation as in [16] and [17], i.e. analog SI cancellation and antenna isolation. The combination of NOMA and FD relay is attractive issue in some works [18], [19]. The authors in [18] introduced a FD assisted cooperative NOMA network relying device-to-device. In such model, the near user is equipped with ability of the FD relay to serve the far user. Considering the outage probability performance, the authors in [19] adopted the FD relay in cooperative NOMA to forward signals to the far user and hence the FD NOMA scheme with its superiority is confirmed. Moreover, more performance gain compared to the HD one and such observation is seen in numerical results to evaluate FD operation. Further, in [20] the authors examined energy efficiency, outage probability and ergodic rate by comparing FD and HD modes in cooperative NOMA with the existence or non-existence of direct link between the far user and the base station (BS). This work is also exhibited that FD NOMA is better than HD NOMA in terms of ergodic rate and outage probability at low signal-to-noise ratio (SNR) regime. To maximize the sum throughput in multi-user FD systems, sub-optimal precoding and power allocation algorithm are studied in [21]. In other work, maximization of the overall throughput in such a FD relay network was investigated by enabling FD design in some kinds of networks [22], [23]. The other potential benefits in NOMA deploying FD relays can be found in [24]–[26]. The authors in [24] explored FD multi-carrier NOMA systems, in which subcarrier allocation algorithm design and the optimal power are further studied to achieve maximization of the weighted system throughput. In addition, the ergodic sum rate in a NOMA FD system is investigated in [25]. In the same research direction, NOMA equipping FD relaying is evaluated and assessed optimal power allocation related to the outage probability as in [26]. However, serious problems appeared in FD NOMA systems where against to eavesdropping signals in comparison with conventional HD OMA systems. The main reason is that the potential for signal leakage occurs as the simultaneous downlink and uplink transmissions and the corresponding multiplexing on these users on each sub-carrier. Security is not satisfied in the existing designs of FD-assisted NOMA systems as in [25]. To avoid the transmission outage caused by the unknown jamming, the authors in [26] considered NOMA transmissions interrupted by the eavesdropper performing passive eavesdropping and active jamming simultaneously. In other work, [27] reported secure performance in such an NOMA system with relay selection. The authors in [27] examined the performance of a system where a base station (master node in IoT) transmits confidential signals to two main sensors (so-called NOMA users) in situation existence of an external eavesdropper.

A. MOTIVATION AND CONTRIBUTIONS

The decreasing cost of UAV is resulted by the rapid growth of wireless network technology and the significant innovation of UAV-based manufacturing technology. Recently, many new UAV applications are introduced such as forest fire prevention systems, weather monitoring systems, man-v-machine areas, etc. The UAV-assisted communication network is proposed as one of the most widespread applications of UAV technology [28]. Recently, since UAV-assisted networks provides improved throughput transmission above 10 Gbps, one can achieve millisecond transmission delay and ultra density device connection, such AUV scheme plays an significant role in 5G and beyond [29], [30]. The UAV network coverage expands to 3D interconnection to address the large scale fading for the ultra speed transmission and satisfy rigorous requirements of the future communications. Regarding cellular infrastructure, it is excessive cost and can be extremely difficult to construct of base stations or urban hotspots. Due to convenient deployment, lower cost and high-altitude assisted transmission, the UAV relay-assisted networks could furnish solutions to implement IoT networks and to provided more benefits [31], [32]. In addition, UAV relay-assisted communications are able to alleviate impact of the line of sight (LoS) transmission effect related to the obstruction of buildings, mountains and other obstacles [33], [34].

In 5G systems, the UAV-enabled communication and NOMA are combined as hybrid network to achieve both superior spectral efficiency and the ubiquitous coverage. Due to mobility and such asymmetric channel conditions, the UAV inherently provides the ability to effectively realize performance gains with NOMA. The authors in [35] presented the joint NOMA user pairing, power allocation, and UAV deployment (placement) for UAV-assisted NOMA systems. They derived the optimal problem of power allocation and UAV placement and then maximal sum-rate of the two-user can be achieved and insights into the optimal structure were provided. Most recently, the authors in [36] introduced offloading application with NOMA by employing bit allocation and trajectory optimization framework for UAV systems. In other applications of NOMA, UAV-to-ground links adopting Rician

fading model for the line-of-sight (LoS) along with outage probability (OP) of both ground users with NOMA are studied [37]. For comparison with NOMA, they compared system relying on NONA and that relying on orthogonal multiple access (OMA) [37].

In other circumstance, the Nakagami-*m* channel model is better suitable to forming links between the BS and relay because the propagation meets less scattering and fewer obstacles. Many works indicated that channel fading make significant influence on the performance of UAV systems and performance analysis for Nakagami-*m* fading is certainly required in practice [38]. Reducing multiple types of channel benefits from the different parameter settings in Nakagami-*m* fading channel model. Special cases of Nakagami-*m* fading include Gaussian channel and Rayleigh fading channel. Cooperative NOMA over Nakagami-*m* fading channels is studied in the context of the spectrum-sharing cognitive radio networks [40]. The multiple relay selection scheme implemented in UAV with energy harvesting capabilities is studied in [38], but they did not consider the impact of Nakagami-*m* fading related to multiple antennas equipped at users. Thanks to applying multiple antenna architecture, the system performance can be further improved by diversity reception. Unfortunately, it is very difficult to obtain closed-form of the performance metrics in such a case. Thus, it is very challenging to provide an accurate analysis of the cooperative UAV system with multiple antennas transmission and NOMA.

Fortunately, the excellent works presented in [38], [41] motivated us to study the system model proposed in this contribution. To the best of our knowledge, the performance of two-way NOMA proposed in [41] using Nakagami-*m* fading channels is not researched for the scenario of UAV yet. Additionally, the authors did not investigate the case if multiple antennas and FD in such a UAV relay assisted system over Nakagami-*m* fading channels. Therefore, our paper addresses these concerns including FD, SIC imperfection, multiple antennas design and necessary comparisons. By employing our considered system, it can provide boosting solution in terms of the wireless connectivity and seamless coverage for mobile communication systems. Additionally, low altitude UAV exhibits a short-range line-of-sight (LoS) links which is beneficial to deployment of the ultra-reliable low latency communication (URLLC) applications. More importantly, by exploiting the aerial feature of UAV one can achieve more advantages such as wide-coverage, flexibility, as well as reliability in unusual and confined medias, especially in temporary activities and disaster. The main contributions of this work are as follows:

- The practical scenario in IoT systems is that the group of base stations (BS) intends to communicate with far users equipped with perfect SIC and multiple antenna through the assistance of a common UAV relay, where the direct links do not exist between the BS and users due to some difficulties related to environment or obstacle.
- In practice, perfect SIC does not exist to support destination users detect their signal. The outage probability and throughput performances are evaluated in imperfect SIC situation. Various numerical results indicated the impact of imperfect SIC on the system performance.
- We derived the closed-form expressions of outage probability for the pairs of NOMA users in scenario of UAV relay-assisted IoT systems. We also demonstrate that UAV relay assisted NOMA scheme with FD mode is capable of outperforming that in HD mode in terms of outage probability over Nakagami-*m* fading channels. We observe that when several users' QoS are met at the same time, such networks can offer optimal outage performance.
- Additionally, we analyzed the delay-limited transmission sum throughput to evaluate the overall system performance. It is worth noting that such IoT systems can achieve reasonable outage behavior and it depends on parameters of channel and threshold SNR required.

B. ORGANIZATION

The remainder of the paper is structured as follows. In Section II, we present the UAV system model and formulate the problem with necessary computations in terms of signal to noise ratio (SNR). This is then followed by the main section, i.e. Section III, which provides system performance via two metrics, outage probability and sum throughput. Next, HD mode and sum throughput are described in sections IV and V. Detailed evaluations and numerical simulation results are examined in Section VI, demonstrating the effectiveness of the proposed parameters through comparing various scenarios. We then finally conclude the paper in Section VII.

II. SYSTEM MODEL

The system model is depicted in Fig. 1. It illustrates a scenario in which a group of base stations (BSs) is known as sources intend to communicate with their corresponding users located in far distance. The direct links between sources and destinations are ignored because of very poor channel conditions and/or physical obstructions. In this situation, by enabling FD/HD mode, a common UAV relay can be operational shared by the pairs of sources and destinations. Two sources denoted as S_1 and S_2 are designed to transmit signal to their corresponding destinations, U_1 and U_2 simultaneously. It is worth noting that S_1 and S_2 following the principle of uplink can be organized as a NOMA pair [38] to transmit simultaneously to common UAV relay R. While two users U_1 and U_2 are able to receive their signals using SIC and it is performed by using the principle of downlink NOMA. These links together with their channels experience Nakagami-*m* fading and additive white Gaussian noise (AWGN). The channel coefficient pertaining to the link $S_1 - R, S_2 - R$ are denoted by h_1, h_2 with the fading parameter m. The links $R - U_1, R - U_2$ correspond with channels $\mathbf{g}_1$, and $\mathbf{g}_2$ respectively. For the first hop transmission, Θ_1, Θ_2 are denoted power allocation factors for signal of user U_1, U_2 respectively (These power factors are set as Θ_3, Θ_4 for the second hop). Without loss

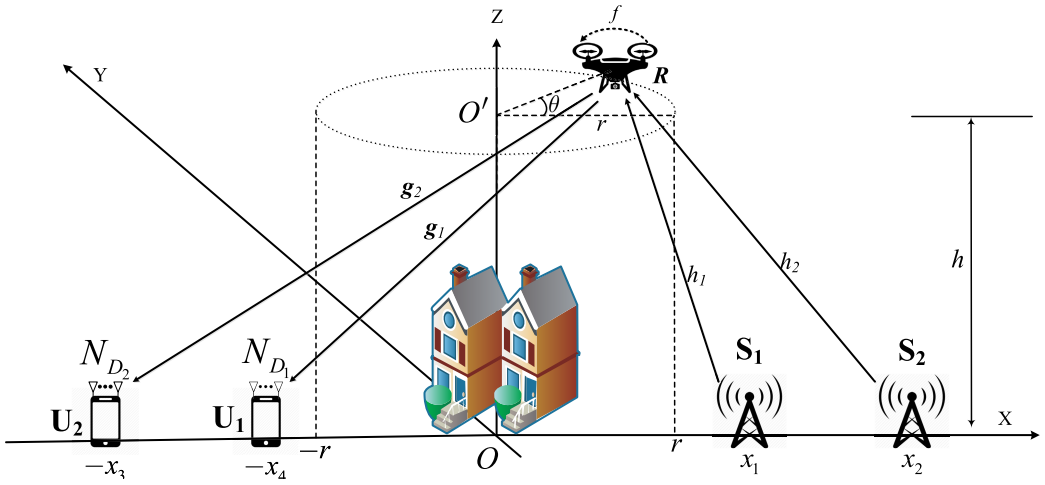

FIGURE 1. System model of UAV relay assisted NOMA system.

of generality, it is assumed that $\Theta_1 > \Theta_2$, $\Theta_3 > \Theta_4$, $\Theta_1+\Theta_2 = 1$ and $\Theta_3+\Theta_4 = 1$. We call P_s, P_r as the transmit power of the source and the relay respectively. Assuming all channel gains experience independent Nakagami-m fading.[1]

In this circumstance, UAV R is designed with fixed-wing [37]. Such UAV continuously flies with set of parameters such as constant velocity v, a circular trajectory of radius r and altitude h. Then, we characterize locations of nodes, i.e. three-dimensional cartesian coordinates $[(x, y, z)$ is used, in which the ground plane is represented by $[(x, y, 0)$ with z as the altitude as shown in Fig. 1. Specifically, we assume the location that the ground sources S_1,S_2 and the users U_1,U_2 are located at $S_1\ (-x_1, 0, 0)$, $S_2\ (-x_2, 0, 0)$, $U_1\ (x_3, 0, 0)$ and $U_2\ (x_4, 0, 0)$, respectively. The centered location of the circular trajectory of UAV R at $O'\ (0, 0, h)$. We denote θ as the angle of the circle of UAV location with respect to x-axis, then the location of R is represented as $R\ (r\cos\theta, r\sin\theta, h)$. Therefore, Euclidean distance from the ground sources S_1,S_2 and the users U_1,U_2 to UAV R can be obtained, respectively as [37]

$$\begin{aligned} d_1 &= \left(h^2 + r^2 + x_1^2 + 2rx_1\cos\theta\right)^{1/2}, \\ d_2 &= \left(h^2 + r^2 + x_2^2 + 2rx_2\cos\theta\right)^{1/2}, \\ d_3 &= \left(h^2 + r^2 + x_3^2 - 2rx_3\cos\theta\right)^{1/2}, \\ d_4 &= \left(h^2 + r^2 + x_4^2 - 2rx_4\cos\theta\right)^{1/2}. \end{aligned} \tag{1}$$

In term of channel distribution, the channel corresponds to its probability density function (PDF) and the cumulative distribution function (CDF) of channel u are given respectively by

$$f_{|u|^2}(x) = \frac{x^{m_u-1}}{\Gamma(m_u)\,\beta_u^{m_u}}\exp\left(-\frac{x}{\beta_u}\right), \tag{2}$$

$$\begin{aligned} F_{|u|^2}(x) &= 1 - \frac{1}{\Gamma(m_u)}\Gamma\left(m_u, \frac{x}{\beta_u}\right) \\ &= 1 - \exp\left(-\frac{x}{\beta_u}\right)\sum_{n=0}^{m_u-1}\frac{x^n}{n!\beta_u^n}, \end{aligned} \tag{3}$$

where $\beta_u \triangleq \lambda_u/m_u$ with λ_u and m_u representing the mean and integer fading factor, respectively. $u \sim \Gamma(m_u, \beta_u)$, $\Gamma(.)$ stands for the Gamma function. It is worth noting that the second line of Eq. (3) holds only when m_u is an integer. Regarding the signal from multiple antennas $f_{\|\mathbf{g}_i\|^2}(y)$ is the PDF and $F_{\|\mathbf{g}_i\|^2}(y)$ is CDF of $\|\mathbf{g}_i\|^2$, given respectively as

$$F_{\|\mathbf{g}_i\|^2}(y) = 1 - e^{-y/\beta_{\mathbf{g}_i}}\sum_{t=0}^{m_iN_{U_i}-1}\frac{y^t}{t!\beta_{\mathbf{g}_i}^t}, \tag{4}$$

$$f_{\|\mathbf{g}_i\|^2}(y) = \sum_{t=0}^{m_iN_{U_i}-1}\frac{1}{t!\beta_{\mathbf{g}_i}^t}\left(\frac{e^{-y/\beta_{\mathbf{g}_i}}}{\beta_{\mathbf{g}_i}}y^t - te^{-y/\beta_{\mathbf{g}_i}}y^{t-1}\right). \tag{5}$$

The SINR to detect x_1 at the relay can be formulated by

$$\gamma_{R\leftarrow 1} = \frac{\Theta_1\rho_s|h_1|^2}{\Theta_2\rho_s|h_2|^2 + \rho_r|f|^2 + 1}. \tag{6}$$

In the HD mode, we have

$$\gamma_{R\leftarrow 1}^{HD} = \frac{\Theta_1\rho_s|h_1|^2}{\Theta_2\rho_s|h_2|^2 + 1}. \tag{7}$$

In a perfect SIC situation, the SINR at the relay to decode x_2 is determined in the FD mode by

$$\gamma_{R\leftarrow 2}^{pSIC} = \frac{\Theta_2\rho_s|h_2|^2}{\rho_r|f|^2 + 1}. \tag{8}$$

While in the HD mode, it can be obtained as

$$\gamma_{R\leftarrow 2}^{pSIC,HD} = \Theta_2\rho_s|h_2|^2. \tag{9}$$

[1]In practical transmission, the obstacles or blockage of urban buildings and mountains lead to block the communication links between source and destinations. Therefore, to realize the transmission process, the UAV relay is necessary to overcome this challenge. It is reasonable to characterize channels between any nodes and the selected UAV relay as Nakagami-m distribution [39].

In other cases, imperfect SIC happens at FD/HD relay, these expressions in terms of SINR can be re-computed respectively as

$$\gamma_{R\leftarrow 2}^{ipSIC} = \frac{\Theta_2 \rho_s |h_2|^2}{\Theta_1 \rho_s |k_r|^2 + \rho_r |f|^2 + 1}, \tag{10}$$

and

$$\gamma_{R\leftarrow 2}^{ipSIC,HD} = \frac{\Theta_2 \rho_s |h_2|^2}{\Theta_1 \rho_s |k_r|^2 + 1}, \tag{11}$$

where $k_r \sim \Gamma\left(m_{k_r}, \beta_{k_r}\right)$ is the interference term related to imperfect SIC, $\rho_s \triangleq P_s/\sigma_0^2$ and $\rho_r \triangleq P_r/\sigma_0^2$ are the transmit SNR of the source and relay nodes, respectively.

The SINR at the destination U_1 in order to decode its own signal can be written by

$$\gamma_{U_1} = \frac{\Theta_3 \rho_r \|\mathbf{g}_1\|^2}{\Theta_4 \rho_r \|\mathbf{g}_1\|^2 + 1}. \tag{12}$$

Additionally, the second user only recovers its data after successfully detecting the first user's data and applying SIC. Then, the SINR at the second user U_2 to detect the first user symbol for SIC purpose and to extract its own signal is given by

$$\gamma_{U_2\leftarrow 1} = \frac{\Theta_3 \rho_r \|\mathbf{g}_2\|^2}{\Theta_4 \rho_r \|\mathbf{g}_2\|^2 + 1}. \tag{13}$$

The SINRs at U_2 in perfect and imperfect SIC are respectively expressed as

$$\gamma_{U_2}^{pSIC} = \Theta_4 \rho_r \|\mathbf{g}_2\|^2, \tag{14}$$

and

$$\gamma_{U_2}^{ipSIC} = \frac{\Theta_4 \rho_r \|\mathbf{g}_2\|^2}{\Theta_3 \rho_r |k_d|^2 + 1}. \tag{15}$$

III. OUTAGE PERFORMANCE IN FD MODE

In this section, we study the outage behavior for the uplink/downlink UAV-based NOMA network with FD relaying. To this end, it needs be derived exact expressions for the outage probability. In order to understand the difficulty in practice regarding SIC, imperfect SIC is further examined.

A. THE OUTAGE PROBABILITY OF THE FIRST USER

In FD mode, we call R_1 and R_2 as target rates for U_1 and U_2, respectively. The outage probability of user U_1 is expressed by

$$\begin{aligned} OP_1^{FD} &= 1 - \Pr\left(\gamma_{R\leftarrow 1} \geq \Xi_0^1, \gamma_{U_1} \geq \Xi_0^1\right) \\ &= 1 - \Pr\left(|h_1|^2 \geq \frac{\Xi_0^1}{\Theta_1 \rho_s}\left(\Theta_2 \rho_s |h_2|^2 + \rho_r |f|^2 + 1\right)\right) \\ &\quad \times \Pr\left(\|\mathbf{g}_1\|^2 \geq \Psi_1\right), \end{aligned} \tag{16}$$

where $\Psi_1 = \frac{\Xi_0^1}{(\Theta_3 - \Im_4 \Xi_0^1)\rho_r}$, $\Xi_0^1 = 2^{R_1} - 1$.

Proposition 1: A closed-form expression of the first user U_1 in term of outage probability can be computed in OP_1^{FD}, as shown at the bottom of the page, where $F_{\|\mathbf{g}_1\|^2}(\Psi_1) = 1 - e^{-\Psi_1/\beta_{\mathbf{g}_1}} \sum_{t=0}^{m_1 N_{U_1} - 1} \frac{\Psi_1^t}{t! \beta_{\mathbf{g}_1}^t}$.

B. THE OUTAGE PROBABILITY OF THE SECOND USER PAIR WITH IMPERFECT SIC

The second user U_2 experiences outage event as follows

$$\begin{aligned} OP_{2,FD}^{ipSIC} &= 1 - \underbrace{\Pr\left(\gamma_{R\leftarrow 1} \geq \Xi_0^1, \gamma_{R\leftarrow 2}^{ipSIC} \geq \Xi_0^2\right)}_{\triangleq \wp_1} \\ &\quad \times \underbrace{\Pr\left(\gamma_{U_2\leftarrow 1} \geq \Xi_0^1, \gamma_{U_2}^{ipSIC} \geq \Xi_0^2\right)}_{\triangleq \wp_2}. \end{aligned} \tag{17}$$

Proposition 2: The closed-form expression of the second user U_2 in term of outage probability can be computed by

$$OP_{2,FD}^{ipSIC} = 1 - \wp_1 \times \wp_2. \tag{18}$$

in which $\wp_1$ computed as (19), shown at the bottom of the next page, and we have

$$\wp_2 = \sum_{t=0}^{m_{g_2} N_{U_2} - 1} \sum_{k=0}^{t} \binom{n}{k} \frac{1}{t!} \left(\frac{\Xi_0^2}{\Theta_4 \beta_{g_2} \rho_r}\right)^t \frac{\Theta_3{}^k \rho_r{}^k e^{-\frac{\Xi_0^2}{\Theta_4 \beta_{g_2} \rho_r}}}{\Gamma\left(m_{k_2}\right) \beta_{k_2}^{m_{k_2}}}$$

$$OP_1^{FD} = 1 - \Pr\left(|h_1|^2 \geq \frac{\Xi_0^1}{\Theta_1 \rho_s}\left(\Theta_2 \rho_s |h_2|^2 + \rho_r |f|^2 + 1\right)\right)\left[1 - F_{\|\mathbf{g}_1\|^2}(\Psi_1)\right]$$

$$= 1 - e^{-\frac{\Xi_0^1}{\Theta_1 \rho_s \beta_{h_1}}} \sum_{n=0}^{m_{h_1}-1} \sum_{n_1=0}^{n} \sum_{n_2=0}^{n_1} \binom{n}{n_1} \binom{n_1}{n_2} \sum_{t=0}^{m_{g1} N_{U_1} - 1} \frac{\rho_r^{n_2}}{n! \beta_{h_1}^n} \left(\frac{\Xi_0^1}{\Theta_1 \rho_s}\right)^n (\Theta_2 \rho_s)^{n_1 - n_2} \Gamma\left(n_2 + m_f\right)$$

$$\times \frac{\Gamma\left(n_1 - n_2 + m_{h_2}\right) e^{-\Psi_1/\beta_{\mathbf{g}_1}}}{\Gamma\left(m_f\right) \Gamma\left(m_{h_2}\right) \beta_f^{m_f} \beta_{h_2}^{m_{h_2}}} \left(\frac{\Xi_0^1 \rho_r}{\Theta_1 \rho_s \beta_{h_1}} + \frac{1}{\beta_f}\right)^{-n_2 - m_f} \left(\frac{\Xi_0^1 \Theta_2}{\Theta_1 \beta_{h_1}} + \frac{1}{\beta_{h_2}}\right)^{-n_1 + n_2 - m_{h_2}} \frac{\Psi_1^t}{t! \beta_{\mathbf{g}_1}^t}.$$

$$\times \left(\frac{\Theta_3 \Xi_0^2 \beta_{\mathbf{g}_2}}{\Theta_4} + \frac{1}{\beta_{k_2}}\right)^{-k-m_{k_2}} \Gamma\left(k + m_{k_2}, \theta\vartheta_2\right) + \sum_{t=0}^{m_{g_2}N_{U_2}-1} \frac{\Psi_1^t e^{-\frac{\Psi_1}{\beta_{g_2}}}}{t!\beta_{g_2}^t} \left(1 - \frac{1}{\Gamma\left(m_{k_2}\right)} \Gamma\left(m_{k_2}, \frac{\vartheta_2}{\beta_{k_2}}\right)\right), \quad (20)$$

where $\theta \triangleq \frac{\Theta_3 \Xi_0^2 \beta_{\mathbf{g}_2}}{\Theta_4} + \frac{1}{\beta_{k_2}}$. $\Gamma(.)$ is the Gamma function and $\Gamma(.,.)$ is the upper incomplete Gamma function.

Proof: See Appendix A. ∎

Remark: It can be seen that expressions of outage performance derived for UAV-aided NOMA system in (6) and (19), the transmit SNR at sources contribute significantly to change expected outage probability. More specifically, the difference in performance comparison of user U_1 and U_1 is resulted from power allocation coefficients. Furthermore, the number of antennas at users leads to adjust outage performance of the considered system.

C. THE OUTAGE PROBABILITY OF THE SECOND USER U_2 IN CASE OF PERFECT SIC

Similarly, for the case of in perfect SIC, the outage probability of the second user U_2 can be formulated by

$$OP_{2,FD}^{pSIC} = 1 - \Pr\begin{pmatrix} \gamma_{R\leftarrow 1} \geq \Xi_0^1, \gamma_{R\leftarrow 2}^{pSIC} \geq \Xi_0^2, \\ \gamma_{U_2\leftarrow 1} \geq \Xi_0^1, \gamma_{U_2}^{pSIC} \geq \Xi_0^2 \end{pmatrix} \quad (21)$$

Proposition 3: The closed-form expression of the second user U_2 in term of outage probability can be given by

$$OP_{2,FD}^{pSIC} = 1 - \underbrace{\Pr\left(\gamma_{R\leftarrow 1} \geq \Xi_0^1, \gamma_{R\leftarrow 2}^{pSIC} \geq \Xi_0^2\right)}_{\wp_3} \times \underbrace{\Pr\left(\gamma_{U_2\leftarrow 1} \geq \Xi_0^1, \gamma_{U_2}^{pSIC} \geq \Xi_0^2\right)}_{\wp_4}. \quad (22)$$

in which $\wp_3$ is computed as in (23), as shown at the bottom of the page, and

$$\wp_4 = e^{-\Psi_2/\beta_{\mathbf{g}_2}} \sum_{t=0}^{m_{g_2}N_{U_2}-1} \frac{\Psi_2^t}{t!\beta_{g_2}^t}. \quad (24)$$

Proof: See Appendix B. ∎

IV. OUTAGE PERFORMANCE IN HD MODE

A. THE OUTAGE PROBABILITY OF THE FIRST USER U_1

The outage probability of the first user U_1 is given by

$$OP_1^{HD} = 1 - \Pr\left(\gamma_{R\leftarrow 1}^{HD} \geq \Xi_{0,HD}^1, \gamma_{U_1} \geq \Xi_{0,HD}^1\right). \quad (25)$$

$\Xi_0^1 = 2^{R_1} - 1$.

Proposition 4: The closed-form expression of the first user U_1 in term of outage probability in HD mode can be given in (26), as shown at the bottom of the next page. Here, we denote $\Xi_0^2 = 2^{R_2} - 1$.

The proof of such proposition is similar, hence we omit it.

B. THE OUTAGE PROBABILITY OF THE SECOND USER U_2 WITH IMPERFECT SIC

In term of imperfect SIC case in HD mode, the outage probability for the second user U_2 can be computed using (27), as shown at the bottom of the next page.

$$\wp_1 = e^{-\frac{\Xi_0^1}{\Theta_1\rho_s\beta_{h_1}} - \left(\frac{\Xi_0^1\Theta_2}{\Theta_1\beta_{h_1}} + \frac{1}{\beta_{h_2}}\right)\frac{\Xi_0^2}{\Theta_2\rho_s}} \sum_{n=0}^{m_{h_1}-1} \sum_{n_1=0}^{n} \sum_{n_2=0}^{n_1} \binom{n}{n_1}\binom{n_1}{n_2} \sum_{n_3=0}^{n_1-n_2+m_{h_2}-1} \sum_{n_4=0}^{n_3} \sum_{n_5=0}^{n_4} \binom{n_3}{n_4}\binom{n_4}{n_5} \frac{1}{n!\beta_{h_1}^n n_3!}$$
$$\times \frac{\rho_r^{n_2}(\Theta_2\rho_s)^{n_1-n_2}\left(n_1 - n_2 + m_{h_2} - 1\right)!}{\Gamma\left(m_{h_2}\right)\Gamma\left(m_f\right)\beta_{h_2}^{m_{h_2}}\beta_f^{m_f}} \left(\frac{\Xi_0^1}{\Theta_1\rho_s}\right)^n \left(\frac{\Xi_0^1\Theta_2}{\Theta_1\beta_{h_1}} + \frac{1}{\beta_{h_2}}\right)^{-n_1+n_2-m_{h_2}} \left[\left(\frac{\Xi_0^1\Theta_2}{\Theta_1\beta_{h_1}} + \frac{1}{\beta_{h_2}}\right)\frac{\Xi_0^2}{\Theta_2\rho_s}\right]^{n_3}$$
$$\times \left[\frac{\Xi_0^1\rho_r}{\Theta_1\rho_s\beta_{h_1}} + \left(\frac{\Xi_0^1\Theta_2}{\Theta_1\beta_{h_1}} + \frac{1}{\beta_{h_2}}\right)\frac{\Xi_0^2\rho_r}{\Theta_2\rho_s} + \frac{1}{\beta_f}\right]^{-n_2-n_4+n_5-m_f} \frac{\rho_r^{n_4-n_5}(\Theta_1\rho_s)^{n_5}}{\Gamma\left(m_{k_r}\right)\beta_{k_r}^{m_{k_r}}} \left[\left(\frac{\Xi_0^1\Theta_2}{\Theta_1\beta_{h_1}} + \frac{1}{\beta_{h_2}}\right)\frac{\Xi_0^2\Theta_1}{\Theta_2} + \frac{1}{\beta_{k_r}}\right]^{-n_5-m_{k_r}}$$
$$\times \Gamma\left(n_2 + n_4 - n_5 + m_f\right)\Gamma\left(n_5 + m_{k_r}\right). \quad (19)$$

$$\wp_3 = \sum_{n=0}^{m_{h_1}-1} \sum_{n_1=0}^{n} \sum_{n_2=0}^{n_1} \sum_{n_3=0}^{n_1-n_2+m_{h_2}-1} \sum_{n_4=0}^{n_3} \binom{n}{n_1}\binom{n_1}{n_2}\binom{n_3}{n_4} \frac{\rho_r^{n_2+n_4}(\Theta_2\rho_s)^{n_1-n_2}\Gamma\left(n_2 + n_4 + m_f\right)\left(n_1 - n_2 + m_{h_2} - 1\right)!}{n!n_3!\beta_{h_1}^n\Gamma\left(m_{h_2}\right)\beta_{h_2}^{m_{h_2}}\Gamma\left(m_f\right)\beta_f^{m_f}}$$
$$\times e^{-\frac{\Xi_0^1}{\Theta_1\rho_s\beta_{h_1}} - \frac{\Xi_0^2}{\Theta_2\rho_s}\left(\frac{\Xi_0^1\Theta_2}{\Theta_1\beta_{h_1}} + \frac{1}{\beta_{h_2}}\right)} \left(\frac{\Xi_0^1}{\Theta_1\rho_s}\right)^n \left[\left(\frac{\Xi_0^1\Theta_2}{\Theta_1\beta_{h_1}} + \frac{1}{\beta_{h_2}}\right)\frac{\Xi_0^2}{\Theta_2\rho_s}\right]^{n_3} \left(\frac{\Xi_0^1\Theta_2}{\Theta_1\beta_{h_1}} + \frac{1}{\beta_{h_2}}\right)^{-n_1+n_2-m_{h_2}}$$
$$\times \left[\frac{\Xi_0^1\rho_r}{\Theta_1\rho_s\beta_{h_1}} + \left(\frac{\Xi_0^1\Theta_2}{\Theta_1} + \frac{1}{\beta_{h_2}}\right)\frac{\Xi_0^2\rho_r}{\Theta_2\rho_s} + \frac{1}{\beta_f}\right]^{-n_2-n_4-m_f}. \quad (23)$$

Proposition 5: The outage probability for the second user U_2 is expressed by

$$OP_{2,HD}^{ipSIC} = 1 - \wp_5 \times \wp_6. \tag{28}$$

in which

$$\begin{aligned}\wp_5 = &\sum_{n=0}^{m_{h_1}-1}\sum_{n_1=0}^{n}\binom{n}{n_1}\sum_{n_2=0}^{\tau_2-1}\sum_{n_3=0}^{n_2}\binom{n_2}{n_3}\\ &\times e^{-\frac{\Xi_{0,HD}^1}{\Theta_1\rho_s\beta_{h_1}}-\frac{\vartheta_{aa}\Xi_{0,HD}^2}{\Theta_2\rho_s}}\frac{\Theta_1^{n_3}\rho_s^{n_3}}{n_2!}\left(\frac{\vartheta_{aa}\Xi_{0,HD}^2}{\Theta_2\rho_s}\right)^{n_2}\\ &\times\frac{\Theta_2^{n_1}}{n!\rho_s^{n-n_1}}\left(\frac{\Xi_{0,HD}^1}{\Theta_1\beta_{h_1}}\right)^{n}\frac{\Gamma(\tau_2)\,\vartheta_{aa}{}^{-\tau_2}}{\Gamma(m_{h_2})\,\beta_{h_2}^{m_{h_2}}}\\ &\times\frac{\Gamma(n_3+m_{k_r})}{\Gamma(m_{k_r})\,\beta_{k_r}^{m_{k_r}}}\left(\frac{\Theta_1\vartheta_{aa}\Xi_{0,HD}^2}{\Theta_2}+\frac{1}{\beta_{k_r}}\right)^{-n_3-m_{k_r}}.\end{aligned} \tag{29}$$

and

$$\begin{aligned}\wp_6 = &\frac{e^{-\frac{\Xi_{0,HD}^2}{\Theta_4\rho_r\beta_{g_2}}}}{\Gamma(m_{k_2})\,\beta_{k_2}^{m_{k_2}}}\sum_{t=0}^{m_{g_2}N_{U_2}-1}\sum_{k=0}^{t}\binom{n}{k}\\ &\times\frac{\Theta_3{}^k\rho_r{}^k}{t!}\left(\frac{\Xi_{0,HD}^2}{\Theta_4\rho_r\beta_{g_2}}\right)^{t}\left(\frac{\Theta_3\Xi_{0,HD}^2}{\Theta_4\beta_{\mathbf{g}_2}}+\frac{1}{\beta_{k_2}}\right)^{-k-m_{k_2}}\\ &\times\Gamma\left(k+m_{k_2},\left(\frac{\Theta_3\Xi_{0,HD}^2}{\Theta_4\beta_{\mathbf{g}_2}}+\frac{1}{\beta_{k_2}}\right)\vartheta_b\right)\\ &+\sum_{t=0}^{m_{g_2}N_{U_2}-1}\frac{\Psi_1^t e^{-\frac{\Psi_1}{\beta_{g_2}}}}{t!\beta_{g_2}^t}\left(1-\frac{1}{\Gamma(m_{k_2})}\Gamma\left(m_{k_2},\frac{\vartheta_b}{\beta_{k_2}}\right)\right).\end{aligned} \tag{30}$$

Proof: See Appendix C. ■

C. THE OUTAGE PROBABILITY OF THE SECOND USER U_2 WITH IMPERFECT SIC

In HD mode, the outage performance of the second user U_2 can be formulated in (31), as shown at the bottom of the page, in which

$$\begin{aligned}\wp_7 = &e^{-\frac{\Xi_{0,HD}^1}{\Theta_1\rho_s\beta_{h_1}}}\sum_{n=0}^{m_{h_1}-1}\sum_{n_1=0}^{n}\binom{n}{n_1}\frac{(\Theta_2\rho_s)^{n_1}}{n!\beta_{h_1}^n}\left(\frac{\Xi_{0,HD}^1}{\Theta_1\rho_s}\right)^{n}\\ &\times\frac{1}{\Gamma(m_{h_2})\,\beta_{h_2}^{m_{h_2}}}\left(\frac{\Xi_{0,HD}^1\Theta_2}{\Theta_1\beta_{h_1}}+\frac{1}{\beta_{h_2}}\right)^{-n_1-m_{h_2}}\\ &\times\Gamma\left(n_1+m_{h_2},\left(\frac{\Xi_{0,HD}^1\Theta_2}{\Theta_1\beta_{h_1}}+\frac{1}{\beta_{h_2}}\right)\frac{\Xi_{0,HD}^2}{\Theta_2\rho_s}\right),\end{aligned} \tag{32}$$

and

$$\wp_8 = e^{-\Psi_b/\beta_{g_2}}\sum_{t=0}^{m_{g_2}N_{U_2}-1}\frac{\Psi_b^t}{t!\beta_{g_2}^t},. \tag{33}$$

where $\Psi_b = \max\left(\Psi_a, \frac{\Xi_{0,HD}^2}{\Theta_4\rho_s}\right)$.

Similarly, the implicit outage derivation in this proposition can be obtained as in the previous proposition. Due to simple analysis, we do not present it here.

V. THROUGHPUT PERFORMANCE

For further evaluation of system, we consider the throughput in delay-limited mode. In particular, the throughput mainly depends on the outage probability.

A. FD MODE

We consider the sum throughput of the system in FD mode in the following cases [43].

$$\begin{aligned}OP_1^{HD} &= 1-\Pr\left(\frac{\Theta_1\rho_s|h_1|^2}{\Theta_2\rho_s|h_2|^2+1}\geq\Xi_{0,HD}^1,\frac{\Theta_3\rho_r\|\mathbf{g}_1\|^2}{\Theta_4\rho_r\|\mathbf{g}_1\|^2+1}\geq\Xi_{0,HD}^1\right)\\ &= 1-e^{-\frac{\Xi_{0,HD}^1}{\Theta_1\rho_s\beta_{h_1}}}\sum_{n=0}^{m_{h_1}-1}\sum_{n_1=0}^{n}\sum_{t=0}^{m_{g_1}N_{U_1}-1}\binom{n}{n_1}\frac{\Psi_a^t}{n!t!\beta_{g_1}^t}\left(\frac{\Xi_{0,HD}^1}{\Theta_1\rho_s\beta_{h_1}}\right)^{n}\Theta_2^{n_1}\rho_s^{n_1}\\ &\quad\times\frac{e^{-\frac{\Psi_a}{\beta_{g_1}}}}{\Gamma(m_{h_2})\,\beta_{h_2}^{m_{h_2}}}\left(\frac{\Xi_{0,HD}^1\Theta_2}{\Theta_1\beta_{h_1}}+\frac{1}{\beta_{h_2}}\right)^{-n_1-m_{h_2}}\Gamma(n_1+m_{h_2}).\end{aligned} \tag{26}$$

$$OP_{2,HD}^{ipSIC} = 1-\underbrace{\Pr\left(\gamma_{R\leftarrow1}^{HD}\geq\Xi_{0,HD}^1,\gamma_{R\leftarrow2}^{ipSIC,HD}\geq\Xi_{0,HD}^2\right)}_{\triangleq\wp_5}\underbrace{\Pr\left(\gamma_{U_2\leftarrow1}\geq\Xi_{0,HD}^1,\gamma_{U_2}^{ipSIC}\geq\Xi_{0,HD}^2\right)}_{\triangleq\wp_6}. \tag{27}$$

$$OP_{2,HD}^{pSIC} = 1-\underbrace{\Pr\left(\gamma_{R\leftarrow1}^{HD}\geq\Xi_{0,HD}^1,\gamma_{R\leftarrow2}^{pSIC,HD}\geq\Xi_{0,HD}^2\right)}_{\triangleq\wp_7}\underbrace{\Pr\left(\gamma_{U_2\leftarrow1}\geq\Xi_{0,HD}^1,\gamma_{U_2}^{pSIC}\geq\Xi_{0,HD}^2\right)}_{\triangleq\wp_8}. \tag{31}$$

Case 1: imperfect SIC

$$\mathcal{T}_{sum,FD}^{ipSIC} = \left(1 - OP_1^{FD}\right) R_1 + \left(1 - OP_{2,FD}^{ipSIC}\right) R_2. \quad (34)$$

Case 2: perfect SIC

$$\mathcal{T}_{sum,FD}^{pSIC} = \left(1 - OP_1^{FD}\right) R_1 + \left(1 - OP_{2,FD}^{pSIC}\right) R_2. \quad (35)$$

B. HD MODE

Similarly, two cases of sum throughput in delay-limited transmission mode are studied as below.

Case 1: imperfect SIC

$$\mathcal{T}_{sum,HD}^{ipSIC} = \left(1 - OP_1^{HD}\right) R_1 + \left(1 - OP_{2,HD}^{ipSIC}\right) R_2. \quad (36)$$

Case 2: perfect SIC

$$\mathcal{T}_{sum,HD}^{pSIC} = \left(1 - OP_1^{HD}\right) R_1 + \left(1 - OP_{2,HD}^{pSIC}\right) R_2. \quad (37)$$

VI. NUMERICAL RESULTS

In this section, we show the comparisons of UAV relay assisted NOMA network and two metrics are considered over uplink and downlink Nakagami-m fading channels. These performance illustrations with different scenarios related to HD/FD mode are considered. We evaluate the impact of the number of antennas at users to their performance. The simulation parameters are as follows, power allocation factors $\Theta_1 = 0.6$, $\Theta_2 = 0.4$, $\Theta_3 = 0.9$, $\Theta_4 = 0.1$, target rate $R_1 = 0.1$ (bps/Hz), $R_2 = 0.1$ (bps/Hz), $N_{U_1} = N_{U_2} = (1, 3)$. The Nakagami-$m$ fading channel parameters are set as $m = m_{h_1} = m_{h_2} = m_f = m_{k_r} = m_{k_2} = m_{g_1} = m_{g_2} = (1, 3)$, $\alpha = 2$; $\kappa = 0.05$, $\lambda_{h_1} = d_1^{-\alpha}$, $\lambda_{h_2} = d_2^{-\alpha}$, $\lambda_{g_1} = d_3^{-\alpha}$, $\lambda_{g_2} = d_4^{-\alpha}$. Regarding FD mode, we set $\lambda_{k_r} = \kappa\lambda_{h_1}$, $\lambda_{k_2} = \kappa\lambda_{h_2}$, $\lambda_f = 0.03$; $\beta_{h_1} = \frac{\lambda_{h_1}}{m_{h_1}}$, $\beta_{h_2} = \frac{\lambda_{h_2}}{m_{h_2}}$, $\beta_f = \frac{\lambda_f}{m_f}$, $\beta_{g_1} = \frac{\lambda_{g_1}}{m_{g_1}}$, $\beta_{g_2} = \frac{\lambda_{g_2}}{m_{g_2}}$, $\beta_{k_r} = \frac{\lambda_{k_r}}{m_{k_r}}$, $\beta_{k_2} = \frac{\lambda_{k_2}}{m_{k_2}}$. The normalized distances as $h = 1$, $x_1 = x_4 = 1$, $x_2 = x_3 = 2$, the certain range of $\theta = 0$ and circular trajectory of radius $r = 0.9$.

Fig. 2 shows that the system outage performance for different numbers of antennas and different cases of SIC operation and FD mode is examined. It is clear that more antennas equipped at users lead to better outage performance at low region of SNR (ρ less than 15 (dB)); perfect SIC at receiver provides better performance compared with imperfect SIC. It can be intuitively seen that saturation of outage behavior happens as ρ becomes greater than 25 (dB). It is also apparent that the system outage behavior may decrease with ρ growing, the reason is that the system outage probability will increase when the corresponding SINR increases. At high region of ρ each user at both two mode HD/FD exhibits the same performance regardless of the number of antennas. This situation occurs since ρ contributes significantly to outage performance rather than the number of antennas. Specially, the second user in mode of perfect SIC shows nearly the same performance at the entire range of ρ. In contrast, the performance gap between the two cases of the number of antennas can be observed only in the first user. Moreover, tight matching between Monte-Carlo simulations and the analytical simulation to confirm the exactness of our analysis. Similar trends can be considered in Fig. 3 for case of HD transmission mode. The lowest outage performance for the case of the first user equipped with 3 antennas. However, we can not recognized how different the performance of two users in perfect SIC scenario at the point as ρ is greater than 25. Imperfect SIC at the second user degrades its performance significantly at two case of the number of antennas.

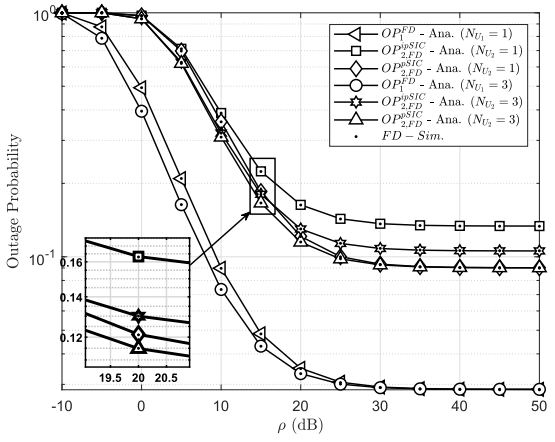

FIGURE 2. Outage probability in FD mode versus ρ with $m = 1$.

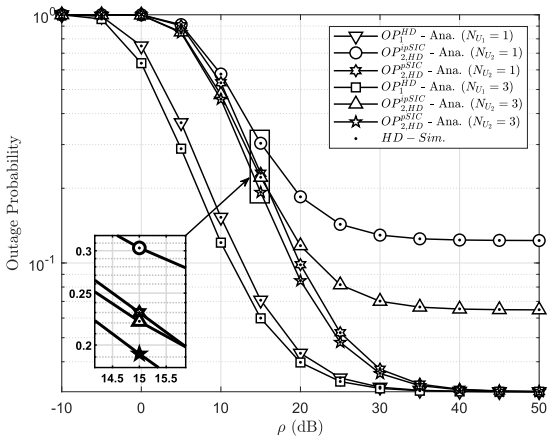

FIGURE 3. Outage probability in HD mode versus ρ with $m = 1$.

Nakagami distribution provides m parameter which describes the fading severity of the propagation channel. In particular, we consider in Fig. 4 the effect of channel fading on the performances of the UAV relay assisted NOMA system by comparing the changes in the metrics for different m parameters. Case $m = 3$ is observed as the better one as comparing performance of each user for $m = 1, 3$. The parameter m is selected to evaluate how seriously channel makes the impact on outage behavior. In addition, such NOMA system in FD mode provides better outage performance compared with that in HD mode. This is due to the fact that there is a loop interference in FD NOMA. Another observation is that HD NOMA and OMA are superior to FD NOMA in the high SNR region. Therefore, we can select different operation

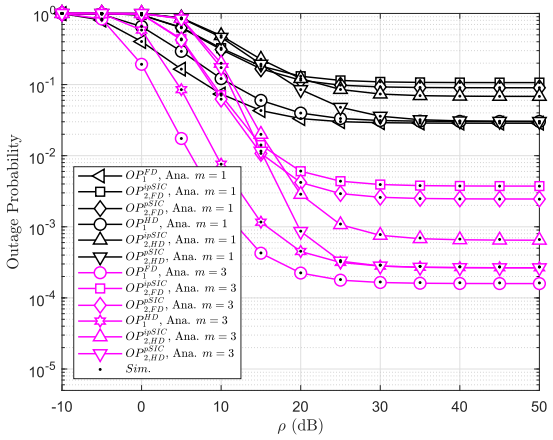

FIGURE 4. Comparison of outage probability with different m fading parameters, with $N_{U_1} = N_{U_2} = 2$.

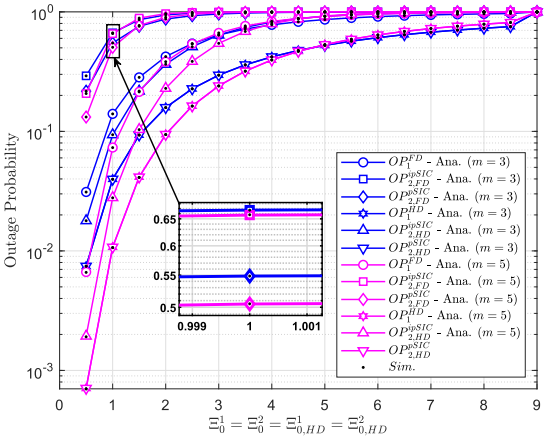

FIGURE 6. Outage probability with $\rho_S = 40\,dB$, $N_{U_1} = N_{U_2} = 3$.

mode for user relaying according to the different SNR levels in practical cooperative NOMA systems.

Fig. 5 depicts how power allocation factors make influence on the outage behavior of each user. It can be intuitively seen that optimal outage performance at the second user as $\Theta_1 = \Theta_3 = 0.55$ for HD mode with imperfect SIC case, as $\Theta_1 = \Theta_3 = 0.45$ for FD mode with imperfect SIC case. While increasing $\Theta_1 = \Theta_3$ results in improving outage performance of the first user. Conditions on such outage event are complicated because they are related to many parameters. These observations can be explained by the fact that SINR terms depend on power allocation factors and hence the corresponding outage probability will be changed.

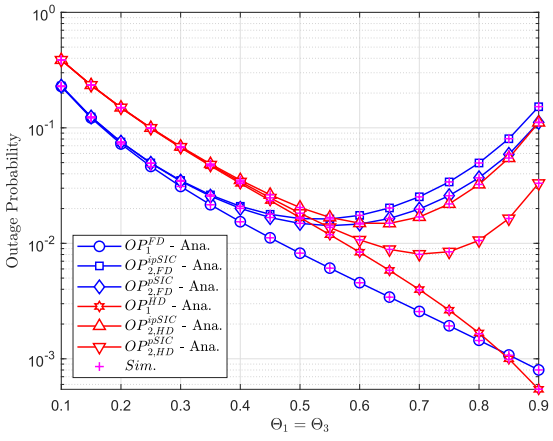

FIGURE 5. Outage probability versus power allocation factors with $\rho_S = 20\,dB$, $N_{U_1} = N_{U_2} = 3$ and $m = 2$.

We also analyze in Fig. 6 the outage performance comparison of this UAV relay assisted NOMA network by varying the threshold SNR with two cases of fading parameters $m = 1, 3$. It can be seen that higher threshold SNR limits the outage performance. Improved outage performance can be noticed at the first user in both FD and HD modes when $m = 3$. In general, when increasing the threshold SNR, the outage performance of such network will be worse.

Fig. 7 illustrates the sum throughput as a function of the SNR ρ. Such sum throughput only increases very fast at low region of ρ. The varying outage probability leads to varying throughput. Therefore, as characteristic of outage behavior at high ρ, the corresponding sum throughput saturates at high ρ as well.

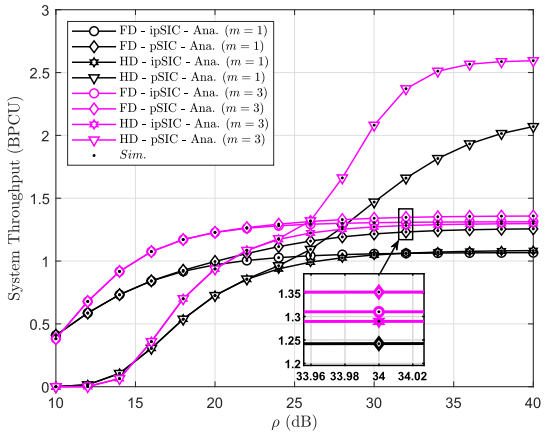

FIGURE 7. The sum throughput of the system in FD/HD under impact of ipSIC and pSIC with $N_{U_1} = N_{U_2} = 3$, $\Theta_1 = \Theta_3 = 0.9$, $R_1 = R_2 = 1.5$ bps/Hz.

In Fig. 8, we analyze the outage probability of different locations of UAV for considered case of FD/HD and pSIC/ipSIC. From this figure, we can see that the unchanged outage performance of the second user occurs in HD mode for both pSIC and ipSIC cases. In contrast, the considered system meets optimal outage probability for FD mode at $\theta = 0$, which means that by adjusting locations of the UAV we can the optimal performance for specific cases. This is because the SINRs depend on channel gains while these channels are related to distance from one node to another node. In addition, the outage probability of system is affected by such SINRs.

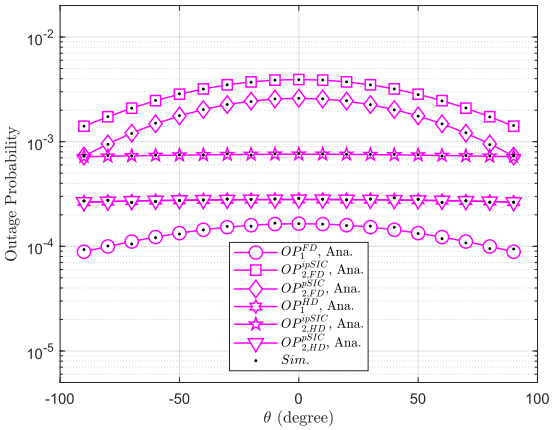

FIGURE 8. Outage probability versus θ, with $m = 3$, $\rho_S = 30\,dB$ and $N_{U_1} = N_{U_2} = 2$.

In Fig. 9, we set simulation parameters as [38], the outage probability of energy harvesting-based NOMA system decreases significantly at high SNR region. Such trends in term of outage performance are same for both time switching and power splitting schemes which are similar our results. However, target rates are still limitations of outage performance of our proposed system and result in [38]. It is concluded that our UAV based NOMA system exhibits the better outage performance in the case of time switching energy harvesting than that in [38] as whole range of SNR.

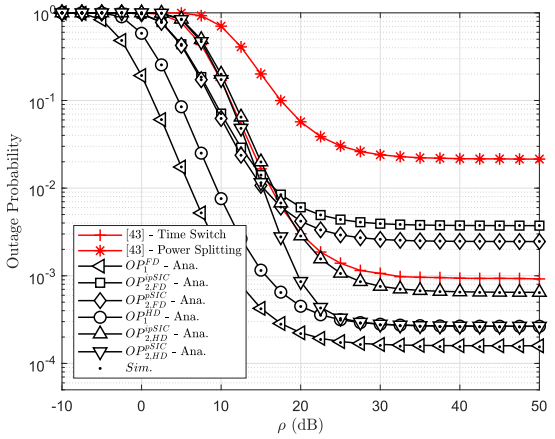

FIGURE 9. A comparison with result reported in [38] in term of outage probability, with $m = 3$, $\rho_S = 30\,dB$ and $N_{U_1} = N_{U_2} = 2$.

VII. CONCLUSION

In this article, a uplink/downlink architecture together with UAV relay benefit to NOMA scheme and UAV-based NOMA system is introduced. Compared with the HD mode in such networks, FD mode enables better outage performance at perfect SIC. The numerical results indicate that design of multiple antennas at users significantly improves the outage and throughput performance by further exploiting the diversity gain of multiple antennas. Such UAV system meets some practical conditions such as FD/HD transmission and perfect SIC/imperfect SIC and necessary comparisons on these cases are provided. Further, by adjust locations of UAV, we can achieve optimal outage performance. By exploring these analysis together with benefits from implementing NOMA, the UAV-assisted NOMA network is proved to be a promising technology. For future research, by focusing on NOMA with multiple user pairs, more results could possibly be found out for uplink/downlink architecture.

APPENDIX A
PROOF OF PROPOSITION 2

We have outage event as below

$$\begin{aligned}\wp_1 &= \Pr\left(\gamma_{R\leftarrow 1} \geq \Xi_0^1, \gamma_{R\leftarrow 2}^{ipSIC} \geq \Xi_0^2\right)\\ &= \Pr\left(\begin{array}{l}\frac{\Theta_1\rho_s|h_1|^2}{\Theta_2\rho_s|h_2|^2+\rho_r|f|^2+1} \geq \Xi_0^1,\\ \frac{\Theta_2\rho_s|h_2|^2}{\Theta_1\rho_s|k_r|^2+\rho_r|f|^2+1} \geq \Xi_0^2\end{array}\right)\\ &= \Pr\left(\begin{array}{l}|h_1|^2 \geq \frac{\Xi_0^1}{\Theta_1\rho_s}\left(\Theta_2\rho_s|h_2|^2+\rho_r|f|^2+1\right),\\ |h_2|^2 \geq \frac{\Xi_0^2}{\Theta_2\rho_s}\left(\Theta_1\rho_s|k_r|^2+\rho_r|f|^2+1\right)\end{array}\right)\\ &= \int_K^\infty \int_0^\infty \int_0^\infty \Delta_2(x,y) f_{|h_2|^2}(y) f_{|f|^2}(x) f_{|k_r|^2}(z)\,dxdydz,\end{aligned} \tag{38}$$

where $K \triangleq \frac{\Xi_0^2}{\Theta_2\rho_s}\left(\Theta_1\rho_s z + \rho_r x + 1\right)$ and

$$\begin{aligned}\Delta_2(x,y) &= 1 - F_{|h_1|^2}\left(\frac{\Xi_0^1}{\Theta_1\rho_s}\left(\Theta_2\rho_s y + \rho_r x + 1\right)\right)\\ &= \sum_{n=0}^{m_{h_1}-1}\sum_{n_1=0}^{n}\sum_{n_2=0}^{n_1}\binom{n}{n_1}\binom{n_1}{n_2}\left(\frac{\Xi_0^1}{\Theta_1}\right)^n\\ &\quad\times\frac{x^{n_2}y^{n_1-n_2}\rho_r^{n_2}\Theta_2^{n_1-n_2}}{n!\beta_{h_1}^n\rho_s^{n-n_1+n_2}}e^{-\frac{\Xi_0^1(\Theta_2\rho_s y+\rho_r x+1)}{\Theta_1\rho_s\beta_{h_1}}}.\end{aligned} \tag{39}$$

Fortunately, the last step can be obtained by using result reported in ([37], eq. (1.111)), after some manipulations with the help of ([37], eq. (3.381.3), eq. (3.381.4) and eq. (8.352.2)), then it can be given as

$$\begin{aligned}\wp_1 &= e^{-\frac{\Xi_0^1}{\Theta_1\rho_s\beta_{h_1}}}\sum_{n=0}^{m_{h_1}-1}\sum_{n_1=0}^{n}\sum_{n_2=0}^{n_1}\binom{n}{n_1}\binom{n_1}{n_2}\\ &\quad\times\frac{\rho_r^{n_2}\Theta_2^{n_1-n_2}}{n!\beta_{h_1}^n\rho_s^{n-n_1+n_2}}\left(\frac{\Xi_0^1}{\Theta_1}\right)^n\\ &\quad\times\frac{1}{\Xi\left(m_{k_r}\right)\beta_{k_r}^{m_{k_r}}}\frac{1}{\Gamma\left(m_f\right)\beta_f^{m_f}}\\ &\quad\times\int_0^\infty\int_0^\infty\Delta_3(x,z)\,e^{-x\left(\frac{\Xi_0^1\rho_r}{\Theta_1\rho_s\beta_{h_1}}+\frac{1}{\beta_f}\right)}\\ &\quad\times x^{n_2+m_f-1}e^{-\frac{z}{\beta_{k_r}}}z^{m_{k_r}-1}dxdz,\end{aligned} \tag{40}$$

where

$$\Delta_3(x,z) = \int_{\frac{\Xi_0^2}{\Theta_2\rho_s}(\Theta_1\rho_s z+\rho_r x+1)}^{\infty} e^{-\frac{\Xi_0^1\Theta_2 y}{\Theta_1\beta_{h_1}}} y^{n_1-n_2} f_y(y)\,dy$$
$$= \frac{\Gamma(\tau_1)\,\vartheta_1^{-\tau_1}}{\Gamma(m_{h_2})\,\beta_{h_2}^{m_{h_2}}} e^{-\frac{\vartheta_1\Xi_0^2}{\Theta_2\rho_s}} e^{-\frac{\vartheta_1\Xi_0^2\rho_r x}{\Theta_2\rho_s}} e^{-\frac{\vartheta_1\Xi_0^2\Theta_1 z}{\Theta_2}}$$
$$\times \sum_{n_3=0}^{\tau_1-1}\sum_{n_4=0}^{n_3}\sum_{n_5=0}^{n_4}\binom{n_3}{n_4}\binom{n_4}{n_5}\frac{\rho_r^{n_4-n_5}}{n_3!}$$
$$\times \left(\frac{\vartheta_1\Xi_0^2}{\Theta_2\rho_s}\right)^{n_3}(\Theta_1\rho_s)^{n_5}x^{n_4-n_5}z^{n_5}, \tag{41}$$

and $\tau_1 \triangleq n_1 - n_2 + m_{h_2}$, $\vartheta_1 \triangleq \frac{\Xi_0^1\Theta_2}{\Theta_1\beta_{h_1}} + \frac{1}{\beta_{h_2}}$.

Finally, replacing (41) in (40), it can be achieved $\wp_1$, $\wp_2$ as shown at the bottom of the page

Then, other terms can be given as

$$\varpi_1 = \int_{\vartheta_2}^{\infty}\left(1 - F_{\|\mathbf{g}_2\|^2}\left(\frac{\Xi_0^2}{\Theta_4\rho_r}(\Theta_3\rho_r x+1)\right)\right) f_{|k_2|^2}(x)\,dx$$
$$= \frac{e^{-\frac{\Xi_0^2}{\Theta_4\rho_r\beta_{\mathbf{g}_2}}}}{\Gamma(m_{k_2})\,\beta_{k_2}^{m_{k_2}}} \sum_{t=0}^{m_{g_2}N_{U_2}-1}\sum_{k=0}^{t}\binom{n}{k}\frac{1}{t!}\left(\frac{\Xi_0^2}{\Theta_4\rho_r\beta_{\mathbf{g}_2}}\right)^t$$
$$\times {\Theta_3}^k {\rho_r}^k \int_{\vartheta_2}^{\infty} e^{-\left(\frac{\Theta_3\Xi_0^2}{\Theta_4\beta_{\mathbf{g}_2}}+\frac{1}{\beta_{k_2}}\right)x} x^{k+m_{k_2}-1}dx$$
$$= \frac{e^{-\frac{\Xi_0^2}{\Theta_4\rho_r\beta_{\mathbf{g}_2}}}}{\Gamma(m_{k_2})\,\beta_{k_2}^{m_{k_2}}} \sum_{t=0}^{m_{\mathbf{g}_2}N_{U_2}-1}\sum_{k=0}^{t}\binom{n}{k}\frac{{\Theta_3}^k{\rho_r}^k}{t!}$$
$$\times \left(\frac{\Xi_0^2}{\Theta_4\rho_r\beta_{\mathbf{g}_2}}\right)^t \left(\frac{\Theta_3\Xi_0^2}{\Theta_4\beta_{\mathbf{g}_2}}+\frac{1}{\beta_{k_2}}\right)^{-k-m_{k_2}}$$
$$\times \Gamma\left(k+m_{k_2}, \left(\frac{\Theta_3\Xi_0^2}{\Theta_4\beta_{\mathbf{g}_2}}+\frac{1}{\beta_{k_2}}\right)\vartheta_2\right), \tag{44}$$

and

$$\varpi_2 = \left[1 - F_{\|\mathbf{g}_2\|^2}\left(\frac{\Xi_0^1}{(\Theta_3-\Xi_0^1\Theta_4)\,\rho_r}\right)\right] F_{|k_2|^2}(\vartheta_2)$$
$$= \sum_{t=0}^{m_2N_{U_2}-1}\frac{e^{-\frac{\Psi_1}{\beta_{\mathbf{g}_2}}}\Psi_1^t}{t!\beta_{\mathbf{g}_2}^t}\left[1 - \frac{1}{\Gamma(m_{k_2})}\Gamma\left(m_{k_2}, \frac{\vartheta_2}{\beta_{k_2}}\right)\right]. \tag{45}$$

Substituting (44) and (45), we have

$$\wp_2 = \varpi_1 + \varpi_2$$
$$= \sum_{t=0}^{m_2N_{U_2}-1}\sum_{k=0}^{t}\binom{n}{k}\frac{1}{t!}\left(\frac{\Xi_0^2}{\Theta_4\rho_r\beta_{\mathbf{g}_2}}\right)^t {\Theta_3}^k{\rho_r}^k$$
$$\times \frac{e^{-\frac{\Xi_0^2}{\Theta_4\rho_r\beta_{\mathbf{g}_2}}}}{\Gamma(m_{k_2})\,\beta_{k_2}^{m_{k_2}}}\left(\frac{\Theta_3\Xi_0^2}{\Theta_4\beta_{\mathbf{g}_2}}+\frac{1}{\beta_{k_2}}\right)^{-k-m_{k_2}}$$
$$\times \Gamma\left(k+m_{k_2}, \left(\frac{\Theta_3\Xi_0^2}{\Theta_4\beta_{\mathbf{g}_2}}+\frac{1}{\beta_{k_2}}\right)\vartheta_2\right)$$
$$+ \sum_{t=0}^{m_2N_{U_2}-1}\frac{e^{-\frac{\Psi_1}{\beta_{\mathbf{g}_2}}}\Psi_1^t}{t!\beta_{\mathbf{g}_2}^t}\left[1 - \frac{1}{\Gamma(m_{k_2})}\Gamma\left(m_{k_2}, \frac{\vartheta_2}{\beta_{k_2}}\right)\right], \tag{46}$$

$$\wp_1 = e^{-\frac{\Xi_0^1}{\Theta_1\rho_s\beta_{h_1}}-\left(\frac{\Xi_0^1\Theta_2}{\Theta_1\beta_{h_1}}+\frac{1}{\beta_{h_2}}\right)\frac{\Xi_0^2}{\Theta_2\rho_s}} \sum_{n=0}^{m_{h_1}-1}\sum_{n_1=0}^{n}\sum_{n_2=0}^{n_1}\binom{n}{n_1}\binom{n_1}{n_2}\sum_{n_3=0}^{n_1-n_2+m_{h_2}-1}\sum_{n_4=0}^{n_3}\sum_{n_5=0}^{n_4}\binom{n_3}{n_4}\binom{n_4}{n_5}\frac{1}{n!\beta_{h_1}^n n_3!}$$
$$\times \frac{\rho_r^{n_2}(\Theta_2\rho_s)^{n_1-n_2}(n_1-n_2+m_{h_2}-1)!}{\Gamma(m_{h_2})\,\Gamma(m_f)\,\beta_{h_2}^{m_{h_2}}\beta_f^{m_f}}\left(\frac{\Xi_0^1}{\Theta_1\rho_s}\right)^n\left(\frac{\Xi_0^1\Theta_2}{\Theta_1\beta_{h_1}}+\frac{1}{\beta_{h_2}}\right)^{-n_1+n_2-m_{h_2}}\left[\left(\frac{\Xi_0^1\Theta_2}{\Theta_1\beta_{h_1}}+\frac{1}{\beta_{h_2}}\right)\frac{\Xi_0^2}{\Theta_2\rho_s}\right]^{n_3}$$
$$\times\left[\frac{\Xi_0^1\rho_r}{\Theta_1\rho_s\beta_{h_1}}+\left(\frac{\Xi_0^1\Theta_2}{\Theta_1\beta_{h_1}}+\frac{1}{\beta_{h_2}}\right)\frac{\Xi_0^2\rho_r}{\Theta_2\rho_s}+\frac{1}{\beta_f}\right]^{-n_2-n_4+n_5-m_f}\frac{\rho_r^{n_4-n_5}(\Theta_1\rho_s)^{n_5}}{\Gamma(m_{k_r})\,\beta_{k_r}^{m_{k_r}}}\left[\left(\frac{\Xi_0^1\Theta_2}{\Theta_1\beta_{h_1}}+\frac{1}{\beta_{h_2}}\right)\frac{\Xi_0^2\Theta_1}{\Theta_2}+\frac{1}{\beta_{k_r}}\right]^{-n_5-m_{k_r}}$$
$$\times\Gamma(n_2+n_4-n_5+m_f)\,\Gamma(n_5+m_{k_r}). \tag{42}$$

$$\wp_2 = \Pr\left(\gamma_{U_2\leftarrow 1} \geq \Xi_0^1, \gamma_{U_2}^{ipSIC} \geq \Xi_0^2\right)$$
$$= \Pr\left(\|\mathbf{g}_2\|^2 \geq \max\left(\frac{\Xi_0^1}{(\Theta_3-\Xi_0^1\Theta_4)\,\rho_r}, \frac{\Xi_0^2}{\Theta_4\rho_r}\left(\Theta_3\rho_r|k_2|^2+1\right)\right)\right)$$
$$= \underbrace{\Pr\left(\|\mathbf{g}_2\|^2 \geq \frac{\Xi_0^2}{\Theta_4\rho_r}\left(\Theta_3\rho_r|k_2|^2+1\right), |k_2|^2 > \vartheta_2\right)}_{\triangleq\varpi_1} + \underbrace{\Pr\left(\|\mathbf{g}_2\|^2 \geq \frac{\Xi_0^1}{(\Theta_3-\Xi_0^1\Theta_4)\,\rho_r}, |k_2|^2 \leq \vartheta_2\right)}_{\triangleq\varpi_2}. \tag{43}$$

where $\vartheta_2 = \max\left(0, \frac{1}{\Theta_3\rho_r}\left(\frac{\Theta_4\Xi_0^1}{(\Theta_3-\Xi_0^1\Theta_4)\Xi_0^2}-1\right)\right)$, $\Psi_1 = \frac{\Xi_0^1}{(\Theta_3-\Xi_0^1\Theta_4)\rho_r}$.

This completes the proof.

APPENDIX B
PROOF OF PROPOSITION 3

Similar to the steps in Proof of proposition 2, $\wp_3$ and $\wp_4$ can be calculated as

$$\begin{aligned}\wp_3 &= \Pr\left(\gamma_{R\leftarrow 1} \geq \Xi_0^1, \gamma_{R\leftarrow 2}^{pSIC} \geq \Xi_0^2\right)\\ &= \Pr\left(\frac{\Theta_1\rho_s|h_1|^2}{\Theta_2\rho_s|h_2|^2+\rho_r|f|^2+1} \geq \Xi_0^1, \frac{\Theta_2\rho_s|h_2|^2}{\rho_r|f|^2+1} \geq \Xi_0^2\right)\\ &= \Pr\left(\begin{array}{l}|h_1|^2 \geq \frac{\Xi_0^1}{\Theta_1\rho_s}\left(\Theta_2\rho_s|h_2|^2+\rho_r|f|^2+1\right),\\ |h_2|^2 \geq \frac{\Xi_0^2}{\Theta_2\rho_s}\left(\rho_r|f|^2+1\right)\end{array}\right)\\ &= \int\limits_{\frac{\Xi_0^2}{\Theta_2\rho_s}(\rho_r x+1)}^{\infty}\int\limits_{0}^{\infty}\Delta_4(x,y) f_{|h_2|^2}(y) f_{|f|^2}(x)\,dxdy, \qquad (47)\end{aligned}$$

in which $\Delta_4(x,y)$ can be computed as bottom of the page. It is noted that the last step can be achieved by using trinomial expansion ([42], eq. (1.111)), after some manipulations with the help of ([42], eq. (3.381.3), eq. (3.381.4) and eq. (8.352.2)), we have

$$\begin{aligned}\wp_3 = e^{-\frac{\Xi_0^1}{\Theta_1\rho_s\beta_{h_1}}}&\sum_{n=0}^{m_{h_1}-1}\sum_{n_1=0}^{n}\sum_{n_2=0}^{n_1}\binom{n}{n_1}\binom{n_1}{n_2}\\ &\times\frac{\beta_{k_r}^{-m_{k_r}}\beta_f^{-m_f}\rho_r^{n_2}\Theta_2^{n_1-n_2}}{n!\Gamma\left(m_{k_r}\right)\Gamma\left(m_f\right)\beta_{h_1}^n\rho_s^{n-n_1+n_2}}\left(\frac{\Xi_0^1}{\Theta_1}\right)^n\end{aligned}$$

$$\begin{aligned}\Delta_4(x,y) &= E_{|h_1|^2}\left\{\Pr\left(|h_1|^2 \geq \frac{\Xi_0^1}{\Theta_1\rho_s}\left(\Theta_2\rho_s|h_2|^2+\rho_r|f|^2+1\right)\right)\right\}\\ &= e^{-\frac{\Xi_0^1}{\Theta_1\rho_s\beta_{h_1}}}e^{-\frac{\Xi_0^1\Theta_2\rho_s y}{\Theta_1\rho_s\beta_{h_1}}}e^{-\frac{\Xi_0^1\rho_r x}{\Theta_1\rho_s\beta_{h_1}}}\sum_{n=0}^{m_{h_1}-1}\frac{1}{n!\beta_{h_1}^n}\left(\frac{\Xi_0^1}{\Theta_1\rho_s}\left(\Theta_2\rho_s y+\rho_r x+1\right)\right)^n\\ &= e^{-\frac{\Xi_0^1}{\Theta_1\rho_s\beta_{h_1}}}e^{-\frac{\Xi_0^1\Theta_2\rho_s y}{\Theta_1\rho_s\beta_{h_1}}}e^{-\frac{\Xi_0^1\rho_r x}{\Theta_1\rho_s\beta_{h_1}}}\sum_{n=0}^{m_{h_1}-1}\sum_{n_1=0}^{n}\sum_{n_2=0}^{n_1}\binom{n}{n_1}\binom{n_1}{n_2}\frac{1}{n!\beta_{h_1}^n}\left(\frac{\Xi_0^1}{\Theta_1\rho_s}\right)^n\rho_r^{n_2}(\Theta_2\rho_s)^{n_1-n_2}x^{n_2}y^{n_1-n_2}. \qquad (48)\end{aligned}$$

$$\begin{aligned}\times\int\limits_0^{\infty}\Delta_5(x)\,e^{-x\left(\frac{\Xi_0^1\rho_r}{\Theta_1\rho_s\beta_{h_1}}+\frac{1}{\beta_f}\right)}x^{n_2+m_f-1}dx, \qquad (49)\end{aligned}$$

where

$$\begin{aligned}\Delta_5(x) &= \int\limits_{\frac{\Xi_0^2}{\Theta_2\rho_s}(\rho_r x+1)}^{\infty} e^{-\frac{\Xi_0^1\Theta_2 y}{\Theta_1\beta_{h_1}}}y^{n_1-n_2}f_y(y)\,dy\\ &= \frac{1}{\Gamma\left(m_{h_2}\right)\beta_{h_2}^{m_{h_2}}}\left(\frac{\Xi_0^1\Theta_2}{\Theta_1\beta_{h_1}}+\frac{1}{\beta_{h_2}}\right)^{-n_1+n_2-m_{h_2}}\\ &\times\left(n_1-n_2+m_{h_2}-1\right)!e^{-\left(\frac{\Xi_0^1\Theta_2}{\Theta_1\beta_{h_1}}+\frac{1}{\beta_{h_2}}\right)\frac{\Xi_0^2}{\Theta_2\rho_s}}\\ &\times\sum_{n_3=0}^{n_1-n_2+m_{h_2}-1}\sum_{n_4=0}^{n_3}\binom{n_3}{n_4}\frac{\rho_r^{n_4}}{n_3!}\\ &\times\left(\frac{\Xi_0^2}{\Theta_2\rho_s}\left(\frac{\Xi_0^1\Theta_2}{\Theta_1\beta_{h_1}}+\frac{1}{\beta_{h_2}}\right)\right)^{n_3}\\ &\times e^{-\left(\frac{\Xi_0^1\Theta_2}{\Theta_1\beta_{h_1}}+\frac{1}{\beta_{h_2}}\right)\frac{\Xi_0^2\rho_r x}{\Theta_2\rho_s}}x^{n_4}. \qquad (50)\end{aligned}$$

Finally, plugging (50) into (49), it can be obtained $\wp_3$ in (51), as shown at the bottom of the page.

It is further achieved $\wp_4$ as below

$$\begin{aligned}\wp_4 &= \Pr\left(\gamma_{U_2\leftarrow 1} \geq \Xi_0^1, \gamma_{U_2}^{pSIC} \geq \Xi_0^2\right)\\ &= \Pr\left(\|\mathbf{g}_2\|^2 \geq \max\left(\frac{\Xi_0^1}{\left(\Theta_3-\Xi_0^1\Theta_4\right)\rho_r}, \frac{\Xi_0^2}{\Theta_4\rho_r}\right)\right)\end{aligned}$$

$$\begin{aligned}\wp_3 = &\sum_{n=0}^{m_{h_1}-1}\sum_{n_1=0}^{n}\sum_{n_2=0}^{n_1}\sum_{n_3=0}^{n_1-n_2+m_{h_2}-1}\sum_{n_4=0}^{n_3}\binom{n}{n_1}\binom{n_1}{n_2}\binom{n_3}{n_4}\frac{\rho_r^{n_2+n_4}(\Theta_2\rho_s)^{n_1-n_2}\Gamma\left(n_2+n_4+m_f\right)\left(n_1-n_2+m_{h_2}-1\right)!}{n!n_3!\beta_{h_1}^n\Gamma\left(m_{h_2}\right)\beta_{h_2}^{m_{h_2}}\Gamma\left(m_f\right)\beta_f^{m_f}}\\ &\times e^{-\frac{\Xi_0^1}{\Theta_1\rho_s\beta_{h_1}}-\frac{\Xi_0^2}{\Theta_2\rho_s}\left(\frac{\Xi_0^1\Theta_2}{\Theta_1\beta_{h_1}}+\frac{1}{\beta_{h_2}}\right)}\left(\frac{\Xi_0^1}{\Theta_1\rho_s}\right)^n\left[\left(\frac{\Xi_0^1\Theta_2}{\Theta_1\beta_{h_1}}+\frac{1}{\beta_{h_2}}\right)\frac{\Xi_0^2}{\Theta_2\rho_s}\right]^{n_3}\left(\frac{\Xi_0^1\Theta_2}{\Theta_1\beta_{h_1}}+\frac{1}{\beta_{h_2}}\right)^{-n_1+n_2-m_{h_2}}\\ &\times\left[\frac{\Xi_0^1\rho_r}{\Theta_1\rho_s\beta_{h_1}}+\left(\frac{\Xi_0^1\Theta_2}{\Theta_1}+\frac{1}{\beta_{h_2}}\right)\frac{\Xi_0^2\rho_r}{\Theta_2\rho_s}+\frac{1}{\beta_f}\right]^{-n_2-n_4-m_f}. \qquad (51)\end{aligned}$$

$$= 1 - F_{\|\mathbf{g}_2\|^2}\left(\underbrace{\max\left(\frac{\Xi_0^1}{\left(\Theta_3 - \Xi_0^1\Theta_4\right)\rho_r}, \frac{\Xi_0^2}{\Theta_4\rho_r}\right)}_{\triangleq\Psi_2}\right)$$

$$= e^{-\Psi_2/\beta_{\mathbf{g}_2}} \sum_{t=0}^{m_2 N_{U_2}-1} \frac{\Psi_2^t}{t!\beta_{\mathbf{g}_2}^t}, \tag{52}$$

where $\Psi_2 = \max\left(\frac{\Xi_0^1}{(\Theta_3-\Xi_0^1\Theta_4)\rho_r}, \frac{\Xi_0^2}{\Theta_4\rho_r}\right)$.

It completes the proof.

APPENDIX C
PROOF OF PROPOSITION 5

It can be seen that the outage behavior occurs and depends on some conditions as below

$$\begin{aligned}\wp_5 &= \Pr\left(\gamma_{R\leftarrow 1}^{HD} \geq \Xi_{0,HD}^1, \gamma_{R\leftarrow 2}^{ipSIC,HD} \geq \Xi_{0,HD}^2\right)\\ &= \Pr\left(\frac{\Theta_1\rho_s|h_1|^2}{\Theta_2\rho_s|h_2|^2+1} \geq \Xi_{0,HD}^1, \frac{\Theta_2\rho_s|h_2|^2}{\Theta_1\rho_s|k_r|^2+1} \geq \Xi_{0,HD}^2\right)\\ &= \int_{\frac{\Xi_{0,HD}^2}{\Theta_2\rho_s}(\Theta_1\rho_s z+1)}^{\infty} \Delta_6(y) f_y(y)\, dy \int_0^{\infty} f_z(z)\, dz, \end{aligned} \tag{53}$$

in which

$$\begin{aligned}\Delta_6(y) &= 1 - F_{|h_1|^2}\left(\frac{\Xi_{0,HD}^1}{\Theta_1\rho_s}\left(\Theta_2\rho_s y + 1\right)\right)\\ &= e^{-\frac{\Xi_{0,HD}^1}{\Theta_1\rho_s\beta_{h_1}}} \sum_{n=0}^{m_{h_1}-1}\sum_{n_1=0}^{n}\binom{n}{n_1}\frac{1}{n!}\\ &\quad\times\left(\frac{\Xi_{0,HD}^1}{\Theta_1\rho_s\beta_{h_1}}\right)^n \Theta_2^{n_1}\rho_s^{n_1} e^{-\frac{\Xi_{0,HD}^1\Theta_2}{\Theta_1\beta_{h_1}}y} y^{n_1}. \end{aligned} \tag{54}$$

After making some manipulations with the help of [[42], eq. (3.381.3), eq. (3.381.4) and eq. (8.352.2)], it is given by

$$\begin{aligned}\wp_5 &= e^{-\frac{\Xi_{0,HD}^1}{\Theta_1\rho_s\beta_{h_1}}} \sum_{n=0}^{m_{h_1}-1}\sum_{n_1=0}^{n}\binom{n}{n_1}\frac{\Theta_2^{n_1}}{n!\rho_s^{n-n_1}}\left(\frac{\Xi_{0,HD}^1}{\Theta_1\beta_{h_1}}\right)^n\\ &\quad\times\frac{1}{\Gamma\left(m_{k_r}\right)\beta_{k_r}^{m_{k_r}}}\int_0^{\infty}\Delta_7(z)\, z^{m_{k_r}-1} e^{-\frac{z}{\beta_{k_r}}} dz, \end{aligned} \tag{55}$$

where $\tau_2 = n_1 + m_{h_2}$ and $\vartheta_{aa} = \frac{\Xi_{0,HD}^1\Theta_2}{\Theta_1\beta_{h_1}} + \frac{1}{\beta_{h_2}}$.

Then, $\wp_5$ is rewritten by

$$\begin{aligned}\wp_5 &= e^{-\frac{\Xi_{0,HD}^1}{\Theta_1\rho_s\beta_{h_1}}} \sum_{n=0}^{m_{h_1}-1}\sum_{n_1=0}^{n}\binom{n}{n_1}\frac{\Theta_2^{n_1}}{n!\rho_s^{n-n_1}}\left(\frac{\Xi_{0,HD}^1}{\Theta_1\beta_{h_1}}\right)^n\\ &\quad\times\frac{\Gamma(\tau_2)\,\vartheta_{aa}{}^{-\tau_1}}{\Gamma\left(m_{h_2}\right)\beta_{h_2}^{m_{h_2}}} e^{-\frac{\vartheta_{aa}\Xi_{0,HD}^2}{\Theta_2\rho_s}} \sum_{n_2=0}^{\tau_2-1}\sum_{n_3=0}^{n_2}\binom{n_2}{n_3}\\ &\quad\times\frac{1}{n_2!}\left(\frac{\vartheta_{aa}\Xi_{0,HD}^2}{\Theta_2\rho_s}\right)^{n_2}\Theta_1^{n_3}\rho_s^{n_3}\Gamma\left(n_3+m_{k_r}\right)\\ &\quad\times\frac{1}{\Gamma\left(m_{k_r}\right)\beta_{k_r}^{m_{k_r}}}\left(\frac{\Theta_1\vartheta_{aa}\Xi_{0,HD}^2}{\Theta_2} + \frac{1}{\beta_{k_r}}\right)^{-n_3-m_{k_r}}. \end{aligned} \tag{56}$$

In HD mode, $\wp_6$ can be solved in the same way of $\wp_2$ in FD mode, and hence $\wp_6$ can be written as

$$\begin{aligned}\wp_6 &= \Pr\left(\gamma_{U_2\leftarrow 1} \geq \Xi_{0,HD}^1, \gamma_{U_2}^{ipSIC} \geq \Xi_{0,HD}^2\right)\\ &= e^{-\frac{\Xi_{0,HD}^2}{\Theta_4\rho_r\beta_{\mathbf{g}_2}}}\frac{1}{\Gamma\left(m_{k_2}\right)\beta_{k_2}^{m_{k_2}}}\sum_{t=0}^{m_2N_{U_2}-1}\sum_{k=0}^{t}\binom{n}{k}\frac{1}{t!}\\ &\quad\times{\Theta_3}^k{\rho_r}^k\left(\frac{\Xi_{0,HD}^2}{\Theta_4\rho_r\beta_{\mathbf{g}_2}}\right)^t\left(\frac{\Theta_3\Xi_{0,HD}^2}{\Theta_4\beta_{\mathbf{g}_2}}+\frac{1}{\beta_{k_2}}\right)^{-k-m_{k_2}}\\ &\quad\times\Gamma\left(k+m_{k_2}, \left(\frac{\Theta_3\Xi_{0,HD}^2}{\Theta_4\beta_{\mathbf{g}_2}}+\frac{1}{\beta_{k_2}}\right)\vartheta_b\right)\\ &\quad+e^{-\frac{\Psi_b}{\beta_{\mathbf{g}_2}}}\sum_{t=0}^{m_2N_{U_2}-1}\frac{\Psi_b^t}{t!\beta_{g_2}^t}\left(1-\frac{1}{\Gamma\left(m_{k_2}\right)}\Gamma\left(m_{k_2}, \frac{\vartheta_b}{\beta_{k_2}}\right)\right), \end{aligned} \tag{57}$$

where $\vartheta_b = \max\left(0, \frac{1}{\Theta_3\rho_r}\left(\frac{\Theta_4\Xi_{0,HD}^1}{\left(\Theta_3-\Xi_{0,HD}^1\Theta_4\right)\Xi_{0,HD}^2}-1\right)\right)$,

$\Psi_b = \frac{\Xi_{0,HD}^1}{\left(\Theta_3-\Xi_{0,HD}^1\Theta_4\right)\rho_r}$.

It completes the proof.

REFERENCES

[1] J. G. Andrews, S. Buzzi, W. Choi, S. V. Hanly, A. Lozano, A. C. K. Soong, and J. C. Zhang, "What will 5G be?" *IEEE J. Sel. Areas Commun.*, vol. 32, no. 6, pp. 1065–1082, Jun. 2014.

[2] D.-T. Do, A.-T. Le, and B. M. Lee, "NOMA in cooperative underlay cognitive radio networks under imperfect SIC," *IEEE Access*, vol. 8, pp. 86180–86195, 2020.

[3] D.-T. Do, M.-S.-V. Nguyen, F. Jämeel, R. Jantti, and I. S. Ansari, "Performance evaluation of relay-aided CR-NOMA for beyond 5G communications," *IEEE Access*, vol. 8, pp. 134838–134855, 2020.

[4] D.-T. Do, A.-T. Le, C.-B. Le, and B. M. Lee, "On exact outage and throughput performance of cognitive radio based non-orthogonal multiple access networks with and without D2D link," *Sensors*, vol. 19, no. 15, p. 3314, Jul. 2019.

[5] T.-L. Nguyen and D.-T. Do, "Power allocation schemes for wireless powered NOMA systems with imperfect CSI: An application in multiple antenna-based relay," *Int. J. Commun. Syst.*, vol. 31, no. 15, p. e3789, Oct. 2018.

[6] Z. Shi, H. Wang, Y. Fu, G. Yang, S. Ma, F. Hou, and T. A. Tsiftsis, "Zero-forcing-based downlink virtual MIMO–NOMA communications in IoT networks," *IEEE Internet Things J.*, vol. 7, no. 4, pp. 2716–2737, Apr. 2020.

[7] L. P. Qian, B. Shi, Y. Wu, B. Sun, and D. H. K. Tsang, "NOMA-enabled mobile edge computing for Internet of Things via joint communication and computation resource allocations," *IEEE Internet Things J.*, vol. 7, no. 1, pp. 718–733, Jan. 2020.

[8] Z. Ding, Y. Liu, J. Choi, Q. Sun, M. Elkashlan, I. Chih-Lin, and H. V. Poor, "Application of non-orthogonal multiple access in LTE and 5G networks," *IEEE Commun. Mag.*, vol. 55, no. 2, pp. 185–191, Feb. 2017.

[9] X. Li, M. Zhao, Y. Liu, L. Li, Z. Ding, and A. Nallanathan, "Secrecy analysis of ambient backscatter NOMA systems under I/Q imbalance," *IEEE Trans. Veh. Technol.*, early access, Jul. 2, 2020, doi: 10.1109/TVT.2020.3006478.

[10] X. Li, M. Huang, Y. Liu, V. G Menon, A. Paul, and Z. Ding, "I/Q imbalance aware nonlinear wireless-powered relaying of B5G networks: Security and reliability analysis," 2020, *arXiv:2006.03902*. [Online]. Available: http://arxiv.org/abs/2006.03902
[11] C. Deng, M. Liu, X. Li, and Y. Liu, "Hardware impairments aware full-duplex NOMA networks over rician fading channels," *IEEE Syst. J.*, early access, May 14, 2020, doi: 10.1109/JSYST.2020.2984641.
[12] S. Kalwar, K. Chin, and Z. Yuan, "A hybrid MAC for non-orthogonal multiple access unmanned aerial vehicles networks," *Wireless Netw.*, vol. 26, pp. 3749–3761, Mar. 2020.
[13] X. Li, Q. Wang, Y. Liu, T. A. Tsiftsis, Z. Ding, and A. Nallanathan, "UAV-aided multi-way NOMA networks with residual hardware impairments," *IEEE Wireless Commun. Lett.*, vol. 9, no. 9, pp. 1538–1542, Sep. 2020, doi: 10.1109/LWC.2020.2996782.
[14] D.-T. Do and A.-T. Le, "NOMA based cognitive relaying: Transceiver hardware impairments, relay selection policies and outage performance comparison," *Comput. Commun.*, vol. 146, pp. 144–154, Oct. 2019.
[15] Y. Yuan, Y. Xu, Z. Yang, P. Xu, and Z. Ding, "Energy efficiency optimization in full-duplex user-aided cooperative SWIPT NOMA systems," *IEEE Trans. Commun.*, vol. 67, no. 8, pp. 5753–5767, Aug. 2019.
[16] T. Riihonen, S. Werner, and R. Wichman, "Mitigation of loopback self-interference in full-duplex MIMO relays," *IEEE Trans. Signal Process.*, vol. 59, no. 12, pp. 5983–5993, Dec. 2011.
[17] H. Q. Ngo, H. A. Suraweera, M. Matthaiou, and E. G. Larsson, "Multipair full-duplex relaying with massive arrays and linear processing," *IEEE J. Sel. Areas Commun.*, vol. 32, no. 9, pp. 1721–1737, Sep. 2014.
[18] Z. Zhang, Z. Ma, M. Xiao, Z. Ding, and P. Fan, "Full-duplex device-to-device-aided cooperative non-orthogonal multiple access," *IEEE Trans. Veh. Technol.*, vol. 66, no. 5, pp. 4467–4471, May 2017.
[19] C. Zhong and Z. Zhang, "Non-orthogonal multiple access with cooperative full-duplex relaying," *IEEE Commun. Lett.*, vol. 20, no. 12, pp. 2478–2481, Dec. 2016.
[20] X. Yue, Y. Liu, S. Kang, A. Nallanathan, and Z. Ding, "Exploiting full/half-duplex user relaying in NOMA systems," *IEEE Trans. Commun.*, vol. 66, no. 2, pp. 560–575, Feb. 2018.
[21] D. Nguyen, L.-N. Tran, P. Pirinen, and M. Latva-Aho, "On the spectral efficiency of full-duplex small cell wireless systems," *IEEE Trans. Wireless Commun.*, vol. 13, no. 9, pp. 4896–4910, Sep. 2014.
[22] H.-P. Dang, M.-S. Van Nguyen, D.-T. Do, H.-L. Pham, B. Selim, and G. Kaddoum, "Joint relay selection, full-duplex and device-to-device transmission in wireless powered NOMA networks," *IEEE Access*, vol. 8, pp. 82442–82460, 2020.
[23] D.-T. Do, C.-B. Le, and F. Afghah, "Enabling full-duplex and energy harvesting in uplink and downlink of small-cell network relying on power domain based multiple access," *IEEE Access*, vol. 8, pp. 142772–142784, 2020.
[24] Y. Sun, D. W. K. Ng, Z. Ding, and R. Schober, "Optimal joint power and subcarrier allocation for full-duplex multicarrier non-orthogonal multiple access systems," *IEEE Trans. Commun.*, vol. 65, no. 3, pp. 1077–1091, Mar. 2017.
[25] L. Zhang, J. Liu, M. Xiao, G. Wu, Y.-C. Liang, and S. Li, "Performance analysis and optimization in downlink NOMA systems with cooperative full-duplex relaying," *IEEE J. Sel. Areas Commun.*, vol. 35, no. 10, pp. 2398–2412, Oct. 2017.
[26] L. Lv, Z. Ding, J. Chen, and N. Al-Dhahir, "Design of secure NOMA against full-duplex proactive eavesdropping," *IEEE Wireless Commun. Lett.*, vol. 8, no. 4, pp. 1090–1094, Aug. 2019, doi: 10.1109/LWC.2019.2907852.
[27] D.-T. Do, M.-S. Van Nguyen, T.-A. Hoang, and M. Voznak, "NOMA-assisted multiple access scheme for IoT deployment: Relay selection model and secrecy performance improvement," *Sensors*, vol. 19, no. 3, p. 736, 2019.
[28] Y. Zeng, R. Zhang, and T. J. Lim, "Wireless communications with unmanned aerial vehicles: Opportunities and challenges," *IEEE Commun. Mag.*, vol. 54, no. 5, pp. 36–42, May 2016.
[29] A. Osseiran, F. Boccardi, V. Braun, K. Kusume, P. Marsch, M. Maternia, O. Queseth, M. Schellmann, H. Schotten, H. Taoka, H. Tullberg, M. A. Uusitalo, B. Timus, and M. Fallgren, "Scenarios for 5G mobile and wireless communications: The vision of the METIS project," *IEEE Commun. Mag.*, vol. 52, no. 5, pp. 26–35, May 2014, doi: 10.1109/MCOM.2014.6815890.
[30] B. Ji, Y. Wang, B. Xing, Y. Wang, K. Song, C. Li, and R. Zhao, "Efficient protocol design for device-to-device communication in ultra dense networks," presented at the Int. Symp. Intell. Signal Process. Commun. Syst. (ISPACS), 2017.
[31] L. Gupta, R. Jain, and G. Vaszkun, "Survey of important issues in UAV communication networks," *IEEE Commun. Surveys Tuts.*, vol. 18, no. 2, pp. 1123–1152, 2nd Quart., 2016.
[32] M. Hua, Y. Wang, Z. Zhang, C. Li, Y. Huang, and L. Yang, "Power-efficient communication in UAV-aided wireless sensor networks," *IEEE Commun. Lett.*, vol. 22, no. 6, pp. 1264–1267, Jun. 2018.
[33] Y. Zeng and R. Zhang, "Energy-efficient UAV communication with trajectory optimization," *IEEE Trans. Wireless Commun.*, vol. 16, no. 6, pp. 3747–3760, Jun. 2017.
[34] C. Li, P. Liu, C. Zou, F. Sun, J. M. Cioffi, and L. Yang, "Spectral-efficient cellular communications with coexistent one- and two-hop transmissions," *IEEE Trans. Veh. Technol.*, vol. 65, no. 8, pp. 6765–6772, Aug. 2016.
[35] M. T. Nguyen and L. B. Le, "NOMA user pairing and UAV placement in UAV-based wireless networks," in *Proc. IEEE Int. Conf. Commun. (ICC)*, Shanghai, China, May 2019, pp. 1–6.
[36] S. Jeong, O. Simeone, and J. Kang, "Mobile edge computing via a UAV-mounted cloudlet: Optimization of bit allocation and path planning," 2016, *arXiv:1609.05362*. [Online]. Available: http://arxiv.org/abs/1609.05362
[37] P. K. Sharma and D. I. Kim, "UAV-enabled downlink wireless system with non-orthogonal multiple access," in *Proc. IEEE Globecom Workshops (GC Wkshps)*, Singapore, Dec. 2017, pp. 1–6.
[38] B. Ji, Y. Li, B. Zhou, C. Li, K. Song, and H. Wen, "Performance analysis of UAV relay assisted IoT communication network enhanced with energy harvesting," *IEEE Access*, vol. 7, pp. 38738–38747, 2019.
[39] A. A. Khuwaja, Y. Chen, and G. Zheng, "Effect of user mobility and channel fading on the outage performance of UAV communications," *IEEE Wireless Commun. Lett.*, vol. 9, no. 3, pp. 367–370, Mar. 2020.
[40] L. Lv, Q. Ni, Z. Ding, and J. Chen, "Application of non-orthogonal multiple access in cooperative spectrum-sharing networks over Nakagami-*m* fading channels," *IEEE Trans. Veh. Technol.*, vol. 66, no. 6, pp. 5506–5511, Jun. 2017.
[41] M. F. Kader, S. Y. Shin, and V. C. M. Leung, "Full-duplex non-orthogonal multiple access in cooperative relay sharing for 5G systems," *IEEE Trans. Veh. Technol.*, vol. 67, no. 7, pp. 5831–5840, Jul. 2018.
[42] S. Gradshteyn and I. M. Ryzhik, *Table of Integrals, Series and Products*, 7th ed. New York, NY, USA: Academic, 2007.
[43] S. K. Singh, K. Agrawal, K. Singh, C.-P. Li, and W.-J. Huang, "On UAV selection and position-based throughput maximization in multi-UAV relaying networks," *IEEE Access*, vol. 8, pp. 144039–144050, 2020.

DINH-THUAN DO (Senior Member, IEEE) received the B.S., M.Eng., and Ph.D. degrees in communications engineering from Vietnam National University (VNU-HCM), in 2003, 2007, and 2013, respectively.

Prior to joining Ton Duc Thang University, he was a Senior Engineer with the VinaPhone Mobile Network, from 2003 to 2009. He has published over 75 SCI/SCIE journal articles, one sole author book, and five book chapters. His research interests include signal processing in wireless communications networks, cooperative communications, non-orthogonal multiple access, full-duplex transmission, and energy harvesting. He was recipient of the Golden Globe Award from Vietnam Ministry of Science and Technology in 2015 (Top Ten Excellent Young Scientists Nationwide). He is currently serving as an Associate Editor for six journals, in which main journals are *EURASIP Journal on Wireless Communications and Networking*, *Computer Communications* (Elsevier), and *KSII Transactions on Internet and Information Systems*.

TU-TRINH THI NGUYEN received the B.Sc. degree in electrical-electronics engineering from the Industrial University of Ho Chi Minh City, Vietnam, in 2018. She intends to pursue her study in Ph.D. degree. She is currently working with the WICOM Laboratory, which has led by Dr. Thuan. Her research interests include signal processing in wireless communications networks, NOMA, and relaying networks.

CHI-BAO LE was born in Binh Thuan, Vietnam. He is currently pursuing the master's degree in communications engineering. He is currently a member of the WICOM Laboratory, Industrial University of Ho Chi Minh City, Vietnam. His research interests include NOMA, MIMO, and signal processing in wireless communications networks.

MIROSLAV VOZNAK (Senior Member, IEEE) received the Ph.D. degree in telecommunications from the Faculty of Electrical Engineering and Computer Science, VSB-Technical University of Ostrava, in 2002, and the Habilitation degree in 2009. He was appointed as a Full Professor in electronics and communications technologies in 2017. He is the author or a coauthor of more than 100 articles in SCI/SCIE journals. His research interests include information and communication technologies, especially on quality of service and experience, network security, wireless networks, and big data analytics. He has served as a member of editorial boards for several journals, including *Sensors*, the *Journal of Communications*, *Elektronika Ir Elektrotechnika*, and *Advances in Electrical and Electronic Engineering*.

ZEESHAN KALEEM received the Ph.D. degree in electronics engineering from INHA University, in 2016. He is currently an Assistant Professor with the Electrical and Computer Engineering Department, COMSATS University Islamabad, Wah Campus. He has published over 50 technical journal and conference papers in reputable venues and also holds 20 U.S. and Korean Patents. His current research interests include public safety networks, 5G system testing and development, and unmanned air vehicle (UAV) communications. He received the Research Productivity Award (RPA) awards from the Pakistan Council of Science and Technology (PSCT) from 2016 to 2017 and 2017 to 2018. He also received the National HEC Best Innovator Award for year 2017. He was a co-recipient of the Best Research Proposal Award from SK Telecom, South Korea. He has been serving as an Associate Technical Editor for prestigious journals/magazine, including *IEEE Communications Magazine*, IEEE Access, IEEE Open Journal of the Communications Society (OJ-COMS), *Computers and Electrical Engineering* (Elsevier), *Human-Centric Computing and Information Sciences* (Springer), and *Journal of Information Processing Systems*. He has served/serving as a Guest Editor for Special Issues of IEEE Access, *Sensors*, IEEE/KICS Journal of Communications and Networks, and *Physical Communication*, and also served as TPC for world distinguished conferences such as IEEE VTC, IEEE ICC, and IEEE PIMRC.

KHALED M. RABIE (Senior Member, IEEE) received the B.S. degree (Hons.) from Tripoli University, Libya, in 2008, and the M.Sc. degree and the Ph.D. degree in electrical and electronic engineering from The University of Manchester, Manchester, U.K., in 2010 and 2015, respectively. He joined Manchester Metropolitan University (MMU), U.K., where he is currently an Assistant Professor with the Department of Engineering. He has published more than 130 articles in prestigious journals and international conferences, and serves regularly on the Technical Program Committee of several major IEEE conferences, such as GLOBECOM, ICC, VTC, and so on. His primary research interest includes various aspects of the next-generation wireless communication systems. He is also a Fellow of the U.K. Higher Education Academy (FHEA). He has received numerous awards over the past few years in recognition of his research contributions, including the Best Student Paper Award at the IEEE ISPLC, TX, USA, in 2015, the MMU Outstanding Knowledge Exchange Project Award of 2016, and the IEEE Access Editor of the Month Award for August 2019. He currently serves as an Associate Editor for IEEE Access, an Area Editor for *Physical Communication* (Elsevier), and an Executive Editor for *Transactions on Emerging Telecommunications Technologies* (Wiley).